Lung Carcinogenesis

Chemically induced *in vitro* transformation of human bronchial epithelial cells

Mari Sjøberg

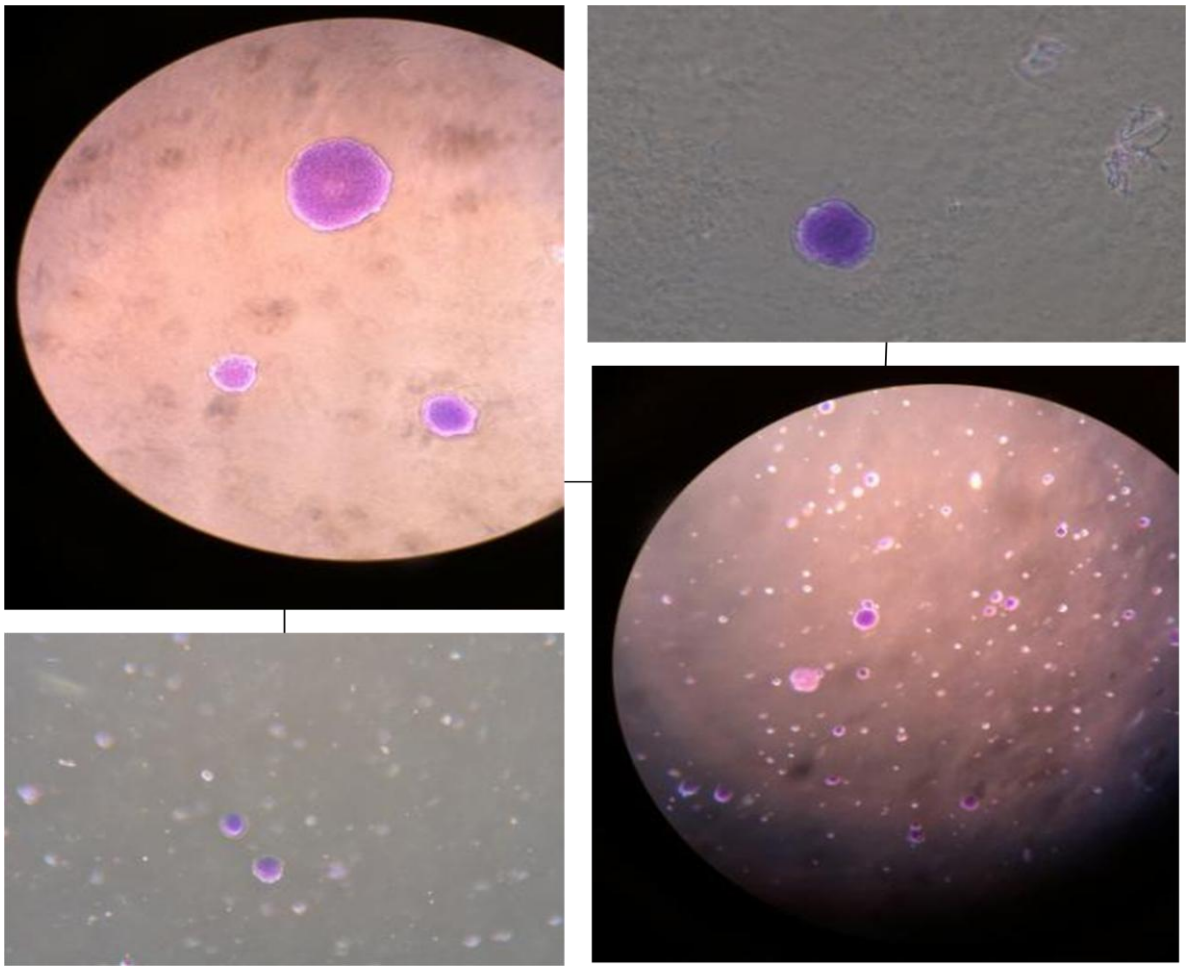

Masteroppgave i toksikologi

Biologisk institutt

Universitetet i Oslo

Juni 2012

Contents

Aknowledgements

The work for this thesis was carried out at the National Institute of Occupational Health, as part of the Master in toxicology (biology) at the University of Oslo. The work at National Institute of Occupational Health started September 2010 and ended May 2012. I would like to thank my supervisors PhD Steen Mollerup and Professor Steinar Øvrebø. Especially, I want to thank Steen Mollerup for good guidance through the work and for his enthusiasm for the project. I also want to thank Audun Bersaas and Rita Bæra for tutoring and patience in the laboratory. A special thank to Audun Bersaas for invaluable support.

Finally, I want to thank the group of toxicology, and everyone who have shown interest and given support for the work for this thesis.

31. Mai 2012

Mari Sjøberg

Abstract

An *in vitro* premalignant transformation model was established to investigate molecular changes during early lung carcinogenesis. hTERT/Cdk4-immortalized human bronchial epithelial cells (HBECs), harboring few genetic alterations, were exposed to tobacco smoke carcinogens (benzo[*a*]pyrene, cigarette smoke condensate, or *N*-methylnitrosourea) for 15 weeks. Transformed cell lines, defined by their ability to form colonies in soft agar, were used as models for molecular investigations, associated with changes in morphology and phenotype. This study shows for the first time that hTERT/Cdk4-immortalized HBECs have the ability to bioactivate the model-PAH, B[*a*]P sufficiently for transformation. Transformed HBECs provided suitable models for further investigations of molecular changes involved in bioactivation and transformation. Transformation was found to be largely associated with changes in cellular morphology from an epithelial to a mesenchymal-like shape. Transformed cells also gained an increased migration capability. These phenotypic changes may characterize an activation of the regulatory, developmental program termed epithelial-to-mesenchymal transition (EMT). This program is important during embryogenesis, but is also activated during cancer progression. Gene expression analyses revealed that the transformed cells also had reduced expression of the E-cadherin-gene (*CDH1*), and an increased expression of the N-cadherin-gene (*CDH2*). This cadherin switch is considered a molecular hallmark of EMT. These results indicate that EMT may also be activated during premalignant transformation.

Steroid receptor signaling pathways have been hypothesized to be involved in lung carcinogenesis, possibly through an interaction with carcinogen metabolism. In this study, increased expression of androgen receptor, estrogen receptor β, and partly also estrogen receptor α was shown to be associated with transformation. This supports the hypothesis of a possible role of steroid receptor pathways during lung carcinogenesis. The forkhead box A (FOXA) transcription factors are involved in regulating steroid receptor activity and may form a link between steroid receptors and carcinogen metabolism. Little is known about these transcription factors in lung cancer. This study shows that the expression of *FOXA1* and *FOXA2* was significantly changed during premalignant transformation. *FOXA2* has been found to act as a suppressor of EMT in

human lung cancer and in this study we observed both a downregulation of *FOXA2* and the E-cadherin-gene (*CDH1*). In conclusion, steroid receptor pathways may be involved in carcinogen induced in vitro transformation of human lung cells, possibly through an interaction with carcinogen metabolism, but also through regulating EMT.

Abbreviations

AHR	Aryl hydrocarbon receptor
ANOVA	Analysis of variance
ARNT	AHR nuclear transferase
B[*a*]p	Benzo[a]pyrene
BPDE	Benzo[a]pyrene diol epoxide
cDNA	Complementary DNA
Cq	Quantification cycle
CSC	Cigarette smoke condensate
CYP	Cytochrome P450
DNA	Deoxyribonucleic acid
DNMT	DNA methyltransferase
EMT	Epithelial-to-mesenchymal transistion
dsRNA	Double stranded RNA
ERE	Estrogen responsive element
FOXA	Forkhead box A
GREB1	Growth regulation by estrogen in breast cancer 1
HBEC	Human bronchial epithelial cells
miRNA	microRNA
mRNA	Messenger RNA
NNK	Nicotine-derived nitrosamine ketone
NNN	N'-nitrosonornicotine
NSCLC	Non-small cell lung cancer
NTC	Non-template control
PAH	Polycyclic aromatic hydrocarbon

qPCR	quantitative polymerase chain reaction
RNA	Ribo nucleic acid
RT-qPCR	Reverse transcriptase quantitative polymerase chain reaction
SCLC	Small cell lung cancer
TERT	Telomerase reverse transcriptase
XRE	Xenobiotic response element

1 Introduction

Cancer is the leading cause of death in economically developed countries and the second leading cause of death in developing countries (Jemal, Bray et al. 2011). The global burden of cancer continues to increase. This is largely because of the aging and growth of the world population, but the adoption of cancer causing behaviors such as smoking, physical inactivity, and westernized diets are also important factors.

Lung cancer is the leading cause of cancer-related deaths worldwide (Parkin, Bray et al. 2005). It was the most commonly diagnosed cancer, as well as the leading cause of cancer deaths in males in 2008. Among females, it was the fourth most commonly diagnosed cancer and the second leading cause of cancer death. (Jemal, Bray et al. 2011)

The relationship between smoking and lung cancer is thoroughly investigated and indicate that smoking is the predominant causal factor for lung cancer (Mattson, Pollack et al. 1987). Due to reductions in the frequency of smokers, both incidence and mortality rates among men have declined, but among women, mortality rates are still increasing (Jemal, Bray et al. 2011). This can mostly be explained by the fact that women started smoking later than men. An increase in tobacco consumption leads to an increase in the incidence of lung cancer a few decades later, but susceptibility factors among women have also been suggested. Epidemiological studies have indicated that women may be at a greater risk of smoking associated lung cancer, compared with men (Zang and Wynder 1996). Both epidemiological and molecular studies indicate that, for a given number of cigarettes smoked, women are at a higher risk of developing lung cancer (Kiyohara and Ohno 2010). Even though it appears that women might be more vulnerable to tobacco carcinogens, some studies indicate that men have a higher rate of fatal outcome of lung cancer (International Early lung cancer program Investigators et al. 2006).

The two major forms of lung cancer are non-small-cell lung cancer (NSCLC), which represents about 85 % of all lung cancers, and small-cell lung cancer (SCLC), accounting for the remaining 15 %. Nearly all patients (over 95%) diagnosed with SCLC are current, or ex-smokers. NSCLC can be divided into adenocarcinoma, squamous cell carcinoma and large cell carcinoma. Adenocarcinomas are the most common type of lung cancer

seen in non-smokers, but smoking has been increasingly associated as a cause in this disease (Youlden, Cramb et al. 2008). There has been a change in histology of lung cancer in which adenocarcinoma has now overtaken squamous cell carcinoma as the most common lung cancer type. This can at least partly be explained by the fact that over the period from 1959 to 1997, concentrations of the cigarette smoke carcinogen nicotine-derived nitrosamine ketone (NNK) increased, while that of benzo[*a*]pyrene (B[*a*]P) decreased. Exposure to NNK has been linked to adenocarcinoma, whereas exposure to B[*a*]P has been linked to squamous cell carcinoma (Hecht 1998).

Despite improvements in survival for many other types of cancer, survival of lung cancer has remained relatively poor. Five years survival of cancers in the breast, colon, and prostate are four to six times longer than that observed for lung cancer (Table 1.1). The high mortality rate from lung cancer is partly due to late diagnosis. NSCLC is often diagnosed at an advanced stage and has poor prognosis. Also, the current lack of effective treatments for advanced lung cancer leads to the high mortality rate. It is assumed that a better understanding of the molecular changes during early lung carcinogenesis can contribute to earlier detection, which may decrease mortality rates. Increased knowledge may also help for the identification of susceptibility factors and the development of more targeted therapies and chemoprevention (Belinsky 2004; Damiani, Yingling et al. 2008).

Table 1.1: Five years survival for key cancers in the United States (Belinsky 2004).

Cancer	New cases	Deaths	5-year survival (%))
Lung	171600	158900	14
Colorectal	129400	56600	63
Breast	176300	43700	85
Prostate	179300	37000	93

1.1 Molecular biology of cancer

Cancer is a broad group of diseases characterized by uncontrolled cell proliferation and tissue invasion. Cancer development is a complex, multistage process driven by the accumulation of genetic and epigenetic changes in genes controlling cell proliferation and tissue homeostasis. Uncontrolled cell proliferation may give the cells a selective growth advantage over adjacent cells. This can lead to the formation of a neoplasm – a new autonomous growth - that proliferates without restraint. As long as this neoplasm is not invasive it is defined as benign, but as it increases in size, so does the possibility of additional critical mutations and/or epigenetic changes in cancer genes. Eventually, the neoplasm can become malignant, invade adjacent tissues and spread into other parts of the body. This last stage of cancer development is termed metastasis (Hanahan and Weinberg 2000; Vogelstein and Kinzler 2004).

There are three types of cancer genes: tumor suppressor genes, oncogenes and stability genes (Vogelstein and Kinzler 2004). Normally, cell proliferation is a strictly regulated process. Proto-oncongenes are normal genes involved in regulation of this process. Activation of proto-oncogenes into oncogenes, by mutations that render the gene constitutively active, often results in increased cell proliferation (Jones and Baylin 2007). Tumor-suppressor genes normally protect against development of neoplasms by regulating the progression through the cell cycle or by inducing apoptosis, when DNA is damaged. Inactivation of tumor suppressor genes results in reduction or loss of function, and may therefore promote cancer development. The third class of cancer genes - stability genes – are involved in DNA repair of mistakes made during replication or after exposure to carcinogens. Mutations in these genes accelerate the carcinogenic process by contributing to more genetic instability (Vogelstein and Kinzler 2004).

Genetic changes are caused by mutations and have traditionally been considered as the major driving mechanism behind cancer development. Epigenetic changes have been given an increasing role and now it is assumed that genetic and epigenetic changes cooperate at all stages of cancer development. Epigenetics can be defined as heritable changes in gene expression that are not accompanied by changes in the DNA sequence (Jones and Baylin 2007). Cancer epigenetics involves mechanisms such as DNA-methylation, histone modification, nucleosome positioning and noncoding RNAs,

specifically microRNA (mi-RNA) expression (Sharma, Kelly et al. 2010) (more on epigenetic mechanisms in cancer, see 1.8).

Epigenetic changes are heritable, but also possibly reversible. The fact that epigenetic changes in theory may be reverted to their normal state by epigenetic therapy makes the field promising and therapeutically relevant.

1.2 The physiological hallmarks of cancer

Molecular changes in cancer genes all operate similarly at the physiological level: by giving the cell certain capabilities that increase cell proliferation and the ability to invade adjacent and distant tissues. Eight physiological capabilities have been described as the hallmarks of cancer (Hanahan and Weinberg 2000; Hanahan and Weinberg 2011). The transformation of normal cells into malignant cancers can be described as a progressive acquisition of an increasing number of these capabilities. The mechanisms behind the acquisition appear to be variable among cancer types.

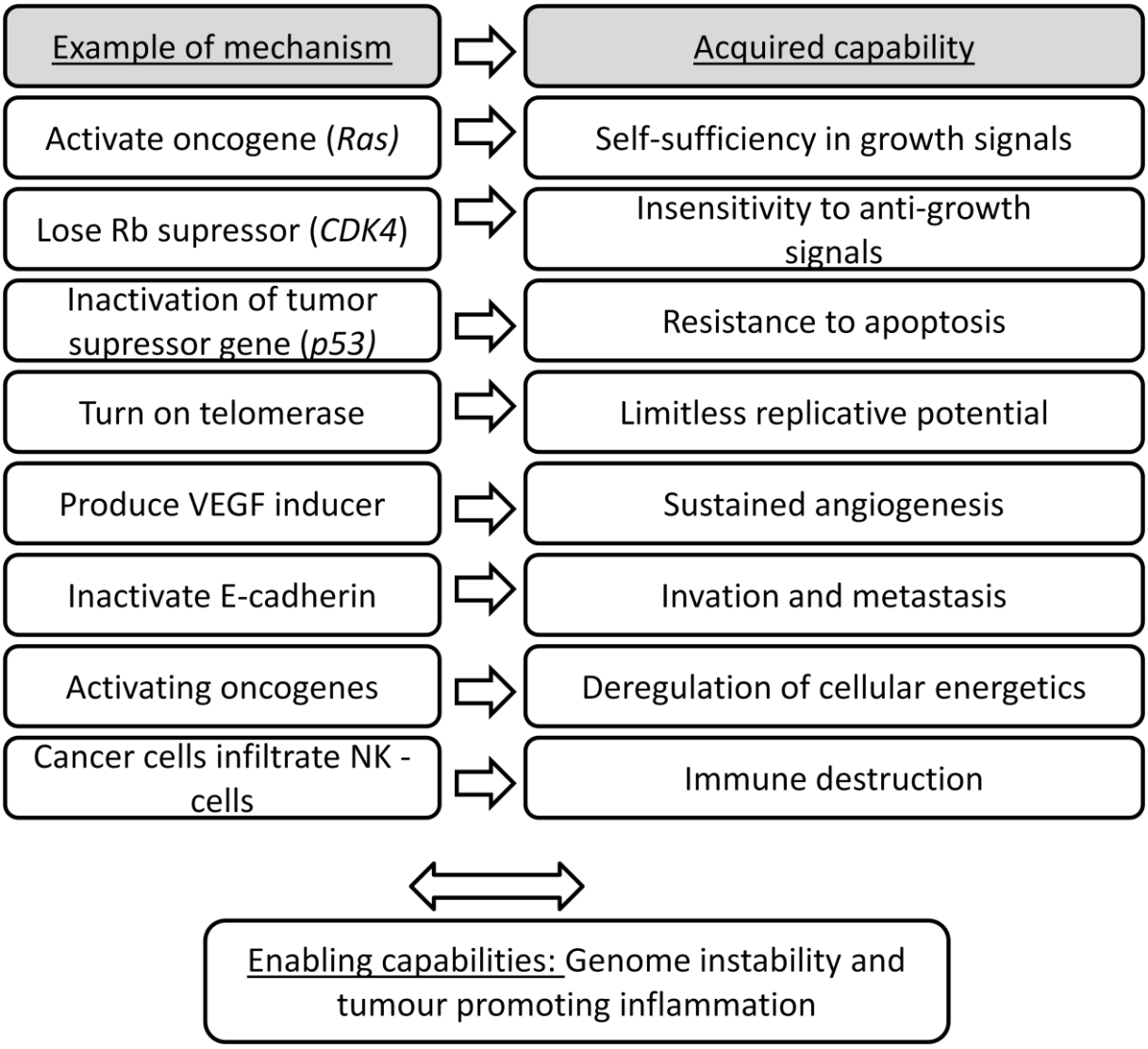

Figure 1.1: The hallmark capabilities of cancer and one example of a mechanism behind the acquisition of each capability. Figure modified from (Hanahan and Weinberg 2011).

Figure 1.1 shows the eight acquired hallmarks capabilities and an example of a mechanism behind. As mentioned, genetic and epigenetic changes that lead to activation of oncogenes or inactivation of tumor suppressor genes are the major mechanisms. Activation of the *Ras* oncogene is a frequent event in many cancers and lead to self-sufficiency in growth signals and uncontrolled cell proliferation. In lung cancer, the *K-Ras* oncogene is mutated in 30-50% of adenocarcinomas (Subramanian and Govindan 2007).

The *p53* tumor suppressor gene has been regarded the "guardian of the genome" and is the most important inducer of apoptosis. Apoptosis (or programmed cell death) is an important response to DNA damage and various physiologic stresses. Apoptosis is

therefore an important tumor suppressing mechanism and resistance to apoptosis is a critical step in cancer development. *p53* also plays an important role in DNA repair and cell cycle arrest. *p53* is mutated in about half of all human cancer cancers and mutations involving *p53* have been reported in 70% of SCLC patients and 50% of NSLC patients (Subramanian and Govindan 2007).

In certain cells, such as stem cells, the enzymes telomerase enzyme hinders the progressive shortening of the ends of chromosomes that otherwise take place during cell replication. This is done by maintaining or extending telomeres. Most normal cell lineages in the body have a finite replicative potential and lack telomerase activity. Replicative cell senescence is also a tumor suppressing mechanism because it counteracts the accumulation of mutations. Limitless replicative potential is a phenotype that is probably acquired during transformation, and activation of the telomerase enzyme is one suggested mechanism (Hanahan and Weinberg 2000).

In the last stage of cancer development, metastasis, cancer cells can escape the primary neoplasm and spread to distant tissues. A developmental regulatory program termed "Epithelial-mesenchymal transition" (EMT) is often activated during this malignant transformation. By activating this program, cells become able to invade and spread to distant tissue to form secondary tumors. One suggested mechanism behind is the inactivation of E-cadherin which is a molecule that form adherence junctions and is important for assembling tissue (For more information on EMT, see 1.7).

1.3 Chemical carcinogenesis

A carcinogen is any chemical, physical or viral agent that causes cancer or increases the risk of developing cancer. Exposure to carcinogens, endogenous or exogenous, induces the genetic and epigenetic changes that may lead to cancer development. Operationally, the multistep carcinogenesis can be divided into three stages, defined as initiation, promotion and progression.

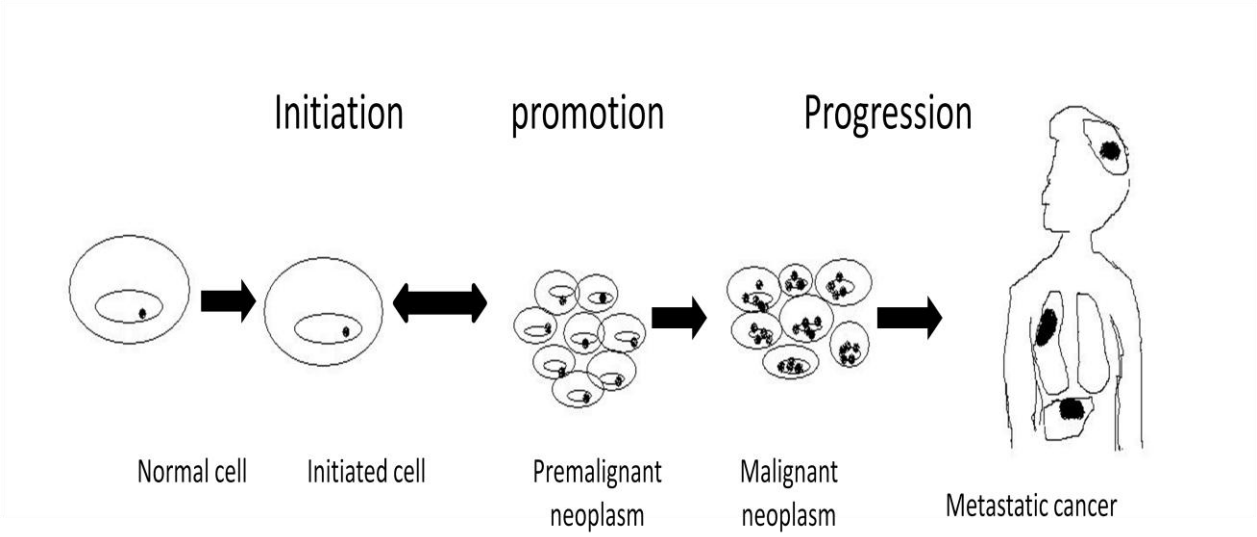

Figure 1.2: Three stage model of carcinogenesis. Figure modified from (Harris 1991).

The first stage, tumor initiation, involves exposure of normal cells to a genotoxic carcinogen that interact physically with DNA to induce a mutation. The initiated cell may, for instance, be less responsive to negative growth factors and inducers of programmed cell death. The initiated cell can have many fates: it can remain in a nondividing state, be deleted through apoptosis, or undergo cell division. If the initiated cell divides, without damage to DNA being repaired, the genetic change is fixed. The next stage, tumor promotion, involves proliferation of the initiated cells to a greater extent than normal, leading to development of a neoplasm. Nongenotoxic carcinogens, called tumor promoters, act at the promotion stage by inducing increased cell proliferation without interacting with the DNA. The promotion stage is therefore reversible. As the neoplasm increases in size, there is an increasing probability of additional genetic damage. This can lead to more genetic and epigenetic changes in cancer genes and the development of malignant neoplasm and metastatic cancer. This final stage of carcinogenesis is called progression and is characterized by genomic instability manifested as an abnormal number and structure of chromosomes, gene amplification, and altered gene expression (Harris 1991)

This simplified three-stage carcinogenesis model demonstrates that carcinogens can play different roles as tumor initiators and tumor promoters. Carcinogens that can act both as tumor initiators (genotoxic) and promoters (nongenotoxic), and thereby induce cancer through all three stages of carcinogenesis are called complete carcinogens. This

three-stage model also demonstrates that the carcinogen induced transformation of normal cells into cancer cells is a stochastic, complex and time consuming process.

1.4 Chemicals in cigarette smoke

Approximately 4000 chemicals have been identified in cigarette smoke and more than 60 of these chemicals have been evaluated by the International Agency for Research on Cancer (IARC) to show sufficient evidence for carcinogenicity in either animals or humans. Chemicals are classified in IARC group 1 when both human and animal data are strong, in group 2A when human epidemiological data are suggestive and animal data strong, and when human epidemiological data are weak but animal data positive, they are classified in group 2B (see Table 1.2)

Experimentally, vapor-phase components of the smoke can be separated from the particulate phase by a glass fiber filter. The vapor-phase consists of nitrogen, oxygen, and carbon dioxide. The particulate phase contains many chemicals including PAH, N-nitrosamines, aromatic amines and metals. Cigarette smoke condensate can be prepared by trapping non- volatile (particulate phase constituents) in cold-traps. Cigarette smoke condensate (CSC) reproducibly causes tumors when applied to mouse skin and implanted in rodent lung. In addition to containing genotoxic compounds, CSC has tumor promoting ability (Pfeifer, Denissenko et al. 2002).

Available data indicate that PAH and NNK are important carcinogens in cigarette smoke most likely to be involved in lung cancer initiation in smokers. It should be noted that some of the strongest carcinogens such as PAH, and NNK are present in lower concentrations and that weaker carcinogens, such as formaldehyde, are present in higher concentrations. PAH are strong locally acting carcinogens and their ability to form tumors has been convincingly established. The model-PAH, B[*a*]P, is a complete carcinogen. NNK are strong systemic lung carcinogens that primarily produce adenocarcinoma.

Table 1.2: The major groups of tobacco smoke carcinogens and the most important within each group. Modified from IARC monograph 83 (2004)

Agent	Notable chemicals	IARC group	Amount in mainstream cigarettes smoke
Polycyclic aromatic hydrocarbons (PAH)	(B[*a*]P	1	8.5- 11.6 ng
N-Nitrosamines	NNK *N*-Nitrosonornicotine (NNN)	1 1	110- 133 ng 154- 196 ng
Aromatic amines	4-Aminobiphenyl 2-Naphtylamine	1 1	2- 5 ng 1-22 ng
Aldehydes	Formaldehyde Acetaldehyde	1 2B	10.3-25 ug 770-864 ug
Volatile hydrocarbons	1,3-butadiene Benzene	2A 1	20-40 ug 12-50 ug
Miscellaneous organic compounds	Ethylene oxide Vinyl chloride	1 1	11-15 ug
Metals	Cadmium Arsenic	1 1	41-62 ng 40-120 ng

1.5 Carcinogen metabolism

When the body is exposed to foreign chemicals, it will try to excrete them by converting them to a more soluble form. The metabolism of foreign compounds is performed by biotransformation enzymes and can be divided into three phases: In phase I (bioactivation), enzymes such as Cytochrome P450 (CYP) introduce reactive or polar groups into the foreign compound to increase water solubility. In phase II (detoxification), these modified compounds are conjugated to polar compounds, which are highly soluble in water. These conjugation-reactions are catalyzed by enzymes such as glutathione *S*-transferase, glucuronosyl-transferase and sulfo-transferase. Finally, in phase III, the conjugated compounds may be further processed and transported out of the cell (Zhang, Wang et al. 2006).

Some of the intermediates formed by the phase l enzymes (bioactivation) are electrophillic and can react with DNA. This can result in the formation of DNA adducts and mutations. Carcinogens can be divided into direct-acting which can induce damage to the DNA directly, and indirect-acting carcinogens that needs to be bioactivated before they can induce DNA damage. Carcinogen bioactivation and the resulting formation of ultimate carcinogens is an inadvertent outcome of the detoxification process.

The human lung is the major target of all inhaled carcinogens, and biotransformation enzymes play a dominant role in the toxicological effect of these carcinogens. The cytochrome P450 family is a large class of enzymes that fulfill many biological functions such as biosynthesis of steroid hormones and biotransformation of chemicals (Zhu 2010). CYP1A1 and CYP1B1 are some of the major isoforms of the CYP enzymes expressed in lung tissue and they play a major role in the bioactivation of B[*a*]P in human lung cell lines (Uppstad, Ovrebo et al. 2010).

The metabolism of B[*a*]P is extensively studied and has served as a model for biotransformation of PAHs. PAHs are important constituents in cigarette smoke, but are also present in broiled foods, soot, tars and automobile exhaust. Figure 1.4 illustrates that B[*a*]P metabolism can follow a detoxifying pathway leading to conjugates that can be excreted, and a bioactivation pathway leading to the formation of the ultimate carcinogen benzo[*a*]pyrene-diol-epoxide (BPDE)(Sagredo, Ovrebo et al. 2006).

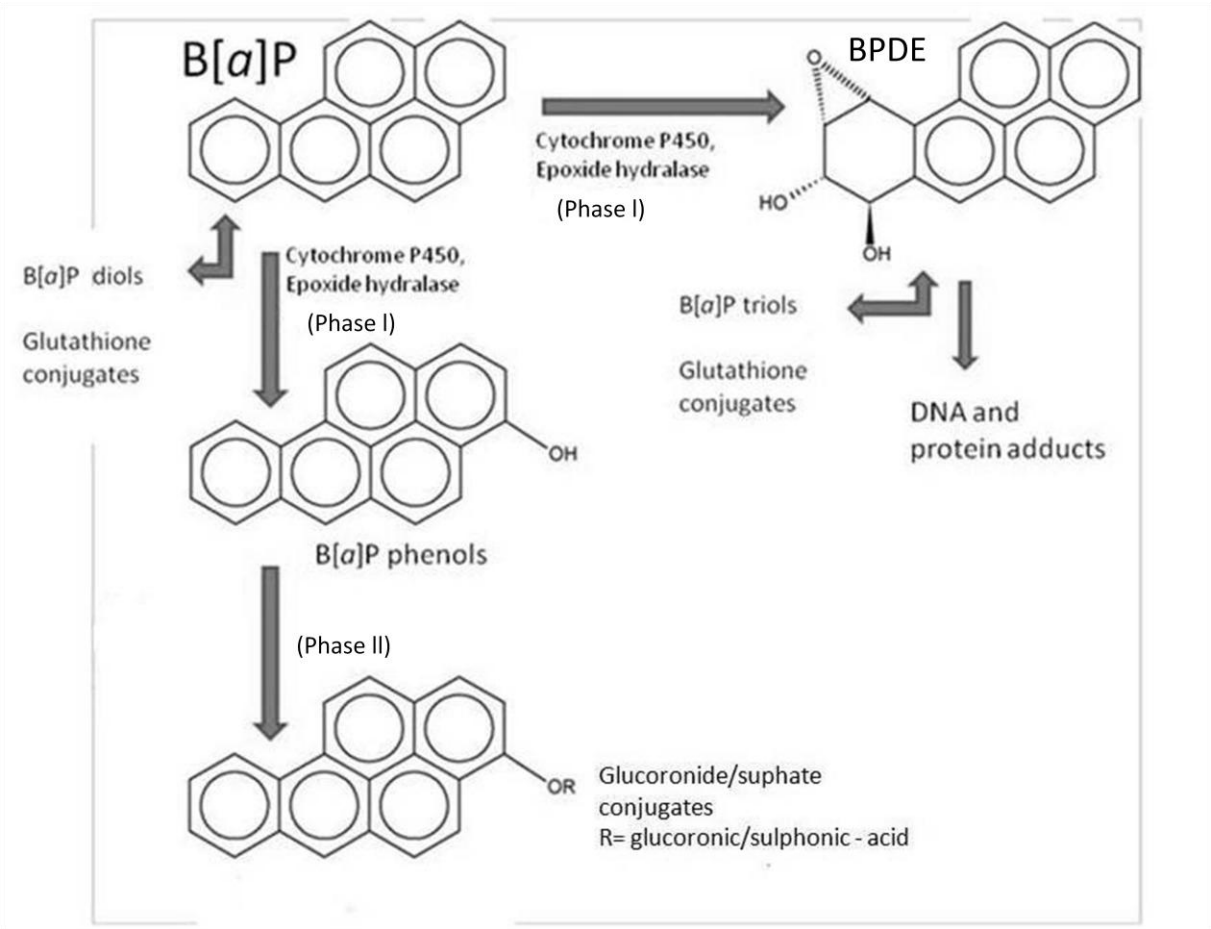

Figure 1.3: B[*a*]P metabolism. Vertical pathway shows detoxification, while horizontal pathway lead to activation and the possible formation of adducts. Figure modified from (Sagredo, Ovrebo et al. 2006).

BPDE is highly reactive and have the ability to form covalent bonds with bases in the DNA molecule, resulting in DNA adducts. Cellular repair systems, such as nucleotide excision repair, eliminates DNA adducts. DNA repair is an important function for maintaining the integrity of the genome and if the adducts escape repair, mutations may arise. The major adduct of BPDE produces GC-TA mutations (Pfeifer, Denissenko et al. 2002). Mutations caused by BPDE adducts *in vitro* are the same that those found in the *p53* gene in tumors from lung cancers. These mutations thereby establish a molecular link between exposure and a specific type of cancer.

Many biotransformation enzymes present in the human lung are inducible by exposure to carcinogens or other foreign compounds. The purpose of enzyme induction is an accelerated metabolism and excretion of the chemicals being exposed. B[*a*]P and other PAHs are primarily bioactivated by CYP1A1 (Uppstad, Ovrebo et al. 2010) which is regulated by the Aryl hydrocarbon receptor (AHR) (Zhu 2010). AHR is a ligand-activated

transcription factor that functions as an intracellular mediator in xenobiotic pathways. AHR also plays an important role in the regulation of cell growth and differentiation. B[*a*]P act as a ligand and bind to the AHR in the cytoplasm (see Fig. 1.4). The liganded AHR is then translocated to the nucleus where it forms a heterodimer with the AHR-nuclear translocator (ARNT). The AHR/ARNT heterodimer recognize and binds to xenobiotic responsive element (XRE) sequences located in the promoter region of several genes such as CYP1A1 and glutathione *S*-transferases. The binding results in transcriptional activation of the genes and induction of phases I and II metabolizing enzymes as well as phase III transporter proteins. (Sagredo, Ovrebo et al. 2006; Zhu 2010)

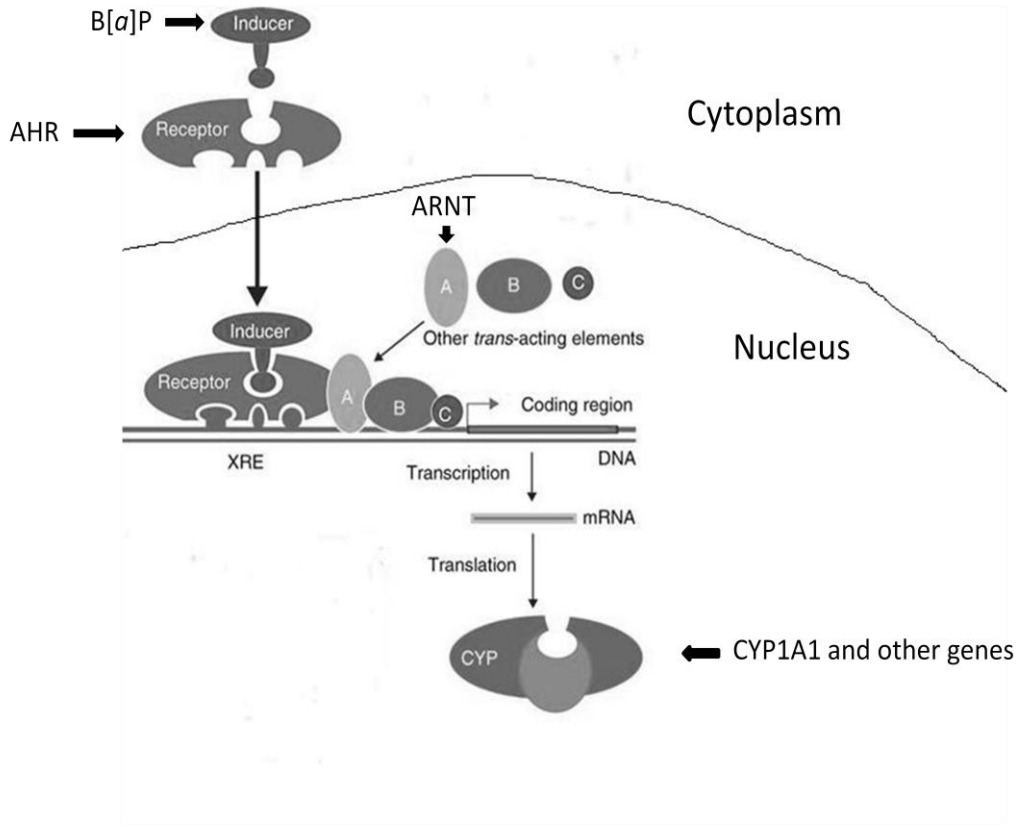

Figure 1.4: An inducer chemical, such as B[*a*]P bind to AHR. This lead to transcription of several genes, including *CYP1A1*, which is necessary for the metabolism of B[*a*]P. Figure modified from (Zhu 2010).

The balance between bioactivation and detoxification varies among individuals and is considered to be important for cancer susceptibility. The level of different biotransformation enzymes is one determining factor and then also the efficiency of

enzyme induction by AHR. A reduction or loss of B[*a*]P carcinogenicity is observed in mice lacking the *Ahr* (Shimizu, Nakatsuru et al. 2000; Sagredo, Mollerup et al. 2009). Upregulation of *CYP1A1* through the AHR and is assumed to increase B[*a*]P carcinogenicity and susceptibility. Higher frequencies of GC-TA transversions in the p53 gene in lung tumors of smoking female lung cancer patient, compared to males, have been observed (Kure, Ryberg et al. 1996). In addition, female lung cancer patients have been found to have a higher level of both *CYP1A1* expression and PAH-DNA adduct levels, compared to men (Mollerup, Ryberg et al. 1999). The level of DNA adducts may be a risk factor for the development of cancer (Veglia, Matullo et al. 2003). Higher frequencies of GC-TA transversions in the p53 gene, which are signatures of PAH-exposure, have also been reported in lung tumors of smoking female lung cancer patients. These findings may indicate higher susceptibility to tobacco smoke carcinogens among females.

1.6 Steroid receptor pathways

Because there are indications of sex differences in susceptibility to tobacco smoke carcinogens, steroid receptors and circulating hormones have been suggested to play a role in lung carcinogenesis. One mechanism may be that circulating hormones interact with receptors in the lung to modulate carcinogen metabolizing enzymes.

Steroids have been implicated as a casual factor in many cancers, such as estrogen and breast cancer. It is well known that estrogen can stimulate cell signaling and proliferation in the breast via Estrogen receptor (ER) pathways and ER independent pathways (Yager and Davidson 2006). In liver cancer, androgens have been suggested as a reason for the sex differences observed in this disease (Li, Tuteja et al. 2012). Androgens have also been found to enhance DNA damage and oxidative stress in liver cancer (Ma et al.,2008). The adult lung is an AR target tissue and there are indications that AR plays a role also in lung cancer biology.

Estrogen regulated gene expression is mediated by the action of two members of the nuclear receptor family, ERα and ERβ. Both normal human lung tissue and lung tumor cell lines have been found to express ERα and ERβ (Mollerup, Jorgensen et al. 2002). A cross-talk between ER and AHR has been observed (Thomsen, Wang et al. 1994; Caruso,

Laird et al. 1999). This may suggest that Estrogen receptor pathways may interact with carcinogen metabolism. Other Studies show that the continued presence of estrogen is required to maintain high levels of AHR expression and thereby the inducibility of *CYP1A1* and *CYP1B1*, in breast cancer cells (Spink, Katz et al. 2003). A similar interaction of AHR and ER in lung carcinogenesis has been suggested and has been hypothesized to at least partly explain sex differences in tobacco carcinogen susceptibility, but this is conflicting (Haugen 2002). One recent study did not support a role of ER in regulation of PAH bioactivation in the human lung (Berge, Mollerup et al. 2004). Other studies indicate that a downregulation of ERα and ERβ, by using siRNA, can affect *CYP1A1* gene expression (Uppstad, Mollerup, unpublished data).

Recently, there has been an increasing focus on genes involved in the activity and regulation of steroid receptors activity. The vertebrate forkhead box A (*FOXA*) gene family of transcription factors are involved in regulation of steroid receptor pathways. They have also been found to be involved in cancer development. The *FOXA* gene family consists of three members: *FOXA1, FOXA2* and *FOXA3* which are encoded by different genes. These are tissue specific transcription factors important during development and differentiation (Lin, Miller et al. 2002. *FOXA1* is important in the regulation of AR and ER activity and several studies indicate that this transcription factor plays a role in several cancer types (Augello, Hickey et al. 2011; Bernardo and Keri 2012). Genome wide location analyses have also revealed that FOXA1 and ERα and AR bind to cis-regulatory elements in their target genes in human breast and prostate cancer cell lines, respectively, and that the recruitment of ERα or AR to their targets, depends on FOXA1. *FOXA1* and *FOXA2* are thought to be important for sexual dimorphism of in liver cancer, where estrogen has a protective effect, and androgen a deleterious effect (Kongsuwan, Knox et al.) In this study, it was also found that the genes regulated by the sex hormone receptors and FOXA factors, clustered in the pathways controlling carcinogen metabolism. Tumor growth was also shown to be strongly dependent on Foxa1/2. Large tumors were found in female Foxa1/2 deficient mouse livers, while tumor growth in male mutants was reduced (Li, Tuteja et al. 2012).

In one study, *FOXA1* was amplified and overexpressed in lung adenocarcinoma (Lin, Miller et al. 2002). *FOXA2,* on the contrary, has recently been found to be

downregulated in lung cancer (Basseres, D'Alò et al.). Little is known about the role of these transcription factors is lung cancer. There are indications that these factors may be involved in regulating carcinogen metabolism (Li, Tuteja et al. 2012), and a recent study also suggest they are involved in regulating EMT (Tang, Shu et al. 2011).

GREB1 (growth regulation by estrogen in breast cancer 1), is critically involved in the estrogen induced growth of breast cancer cells. *GREB1* is characterized as an ERα target gene, with three estrogen response elements (ERE) located on its promoter (Chand, Wijayakumara et al. 2012). Little is known about *GREB1* in lung cancer, but in addition to the FOXA transcription factors, its expression may be indicative of the activity of steroid receptors and may also be involved in lung cancer.

1.7 Epithelial-to-mesenchymal transition (EMT)

Epithelial-to-mesenchymal transition (EMT) is a developmental program that is important in embryogenesis and wound-healing. Activation of this program has been implicated as an important step in cancer invasion and metastasis (Mani, Guo et al. 2008). EMT is characterized by loss of epithelial markers, gain of mesenchymal markers and changes in cellular morphology and phenotype. Through activation of this program, cells acquire an increased ability to migrate and invade other tissues, which are important characteristics during metastasis (Fig 1.5).

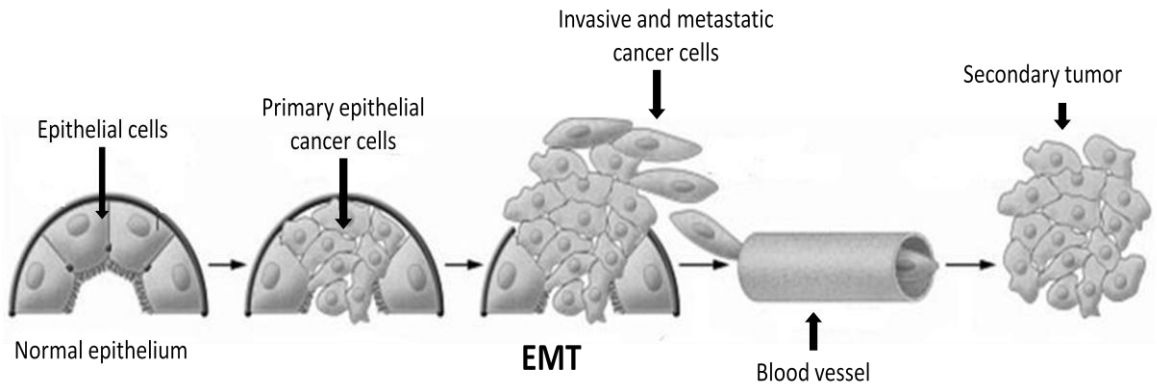

Figure 1.5: Activation of EMT during cancer invasion and metastasis. Figure modified from (Kalluri and Weinberg 2009)

As mentioned earlier, one of the key characteristics of EMT is inactivation of E-cadherin. E-cadherin form adherence junctions with adjacent epithelial cells and thereby helps assemble epithelial tissue. The expression of N-cadherin, on the contrary, is upregulated

during EMT. N-cadherin is normally expressed in migrating neurons and mesenchymal cells during embryogenesis. Downregulation of E-cadherin and upregulation of N-cadherin, often referred to as the cadherin switch, is therefore considered a molecular hallmark of EMT (Kalluri and Weinberg 2009).

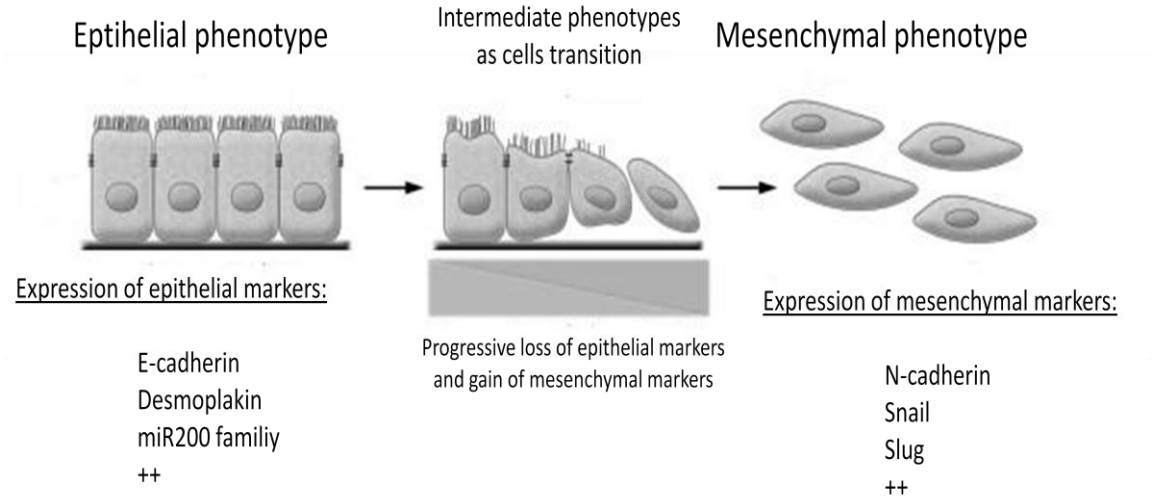

Figure 1.6: Some of the epithelial and mesenchymal markers commonly associated with EMT (Kalluri and Weinberg 2009).

Recent *in vitro* studies indicate that EMT also can be activated in early stages of carcinogenesis. EMT *in vitro* models have been established in both lung and prostate cancer cells. (Ke, Qu et al. 2008). These models allow a clearer identification of the molecular mechanisms of EMT, associated with altered morphology. Recent studies indicate that EMT can be activated in early stages of lung carcinogenesis and that several epigenetic mechanisms are involved. Exposure of human bronchial epithelial cells to tobacco carcinogens induced the EMT- program in a premalignant *in vitro* model. EMT induction was associated with tumor supressive miRNA silencing (Tellez, Juri et al. 2011). Both chromatin remodeling and DNA methylation was involved in the sustained silencing of these miRNAs. One recent study also observed a link between EMT and FOXA1/2 in pancreatic cancer. In this study *FOXA1/2* expression showed a positive regulation of E-cadherin and maintenance of the epithelial phenotype (Song, Washington et al. 2012)

1.8 Epigenetic mechanisms

Among the epigenetic mechanisms involved in cancer, changes in DNA methylation and miRNA expression will be discussed here. DNA methylation is important in regulating many cellular processes and in most cases results in silencing of genes. DNA methylation primarily occurs by the covalent modification of the cytosine bases in CpG dinucleotides. CpG sites are not evenly distributed in the genome. Instead, they are concentrated in CpG rich regions called CpG islands. These CPG Islands are often located in the promoter region of protein coding genes. Their methylation is associated with gene silencing (Sharma, Kelly et al. 2010). In mammalian cells, DNA methylation is carried out by two general classes of enzymatic activities: Maintenance methylation and *de novo* methylation. The enzymes that are responsible for these activities are called DNA methyltransferase (DNMT)(Chuang and Jones 2007). As mentioned previously, inactivation of tumor suppressor genes is an important mechanism behind cancer development and DNA hypermethylation of tumor suppressor genes occurs in many types of cancer. In lung cancer, more than 60 genes have been identified as epigenetically silenced in lung tumors (Belinsky 2004). In one recent study gene promoter hypermethylation mediated by DNMT1 was associated with transformation of immortalized bronchial epithelial cells (Damiani, Yingling et al. 2008).

MicroRNAs are small RNAs (~22 nt) that regulate gene expression by posttranscriptional silencing (Bartel 2009). Sequence-specific base pairing of miRNA with 3` untranslated region (3`-UTR) of mRNA result in mRNA degradation or inhibition of translation (Sharma, Kelly et al. 2010). miRNA seem to have a modest effect on gene regulation with less than 30 % downregulation of most of its targets, but some miRNAs can result in 50-80 % reduction of expression of its mRNA targets (Baek, Villén et al. 2008). Each miRNA can target several mRNAs, and conversely, each mRNA can be targeted by several miRNAs (Enright, John et al. 2003). It has been suggested that miRNA act through fine tuning rather than switching of its targets. miRNA control many biological processes including cell proliferation, apoptosis and differentiation, which also suggest that they may play a role as tumor suppressor genes or oncogenes. Generally, the expression of miRNAs is found to be downregulated in cancer cells, but a few miRNAs have been found to be upregulated (Lynam-Lennon, Maher et al. 2009; Martello, Rosato et al. 2010).

MiR-21 is one of the most studied miRNAs in cancers. MiR-21 is overexpressed in the most solid tumors, promoting progression and metastasis (Tian, Tu et al. 2012).

1.9 Human bronchial epithelial cell lines for *in vitro* studies.

Primary bronchial epithelial cells have a finite replicative potential. This is partly due to lack of telomerase activity and shortening of telomeres. For the use in *in vitro* studies, cell lines are therefore immortalized. Immortality can be accomplished by introduction of oncogenes or silencing of tumor suppressor genes. One way to induce immortality is through viral-mediated induction of viral onco-proteins, but such attempts to establish long-term replicating cultures have generated variants which may become spontaneously transformed (or malignant) after many passages. These cells are often genomically unstable and the *p53* gene has often been inactivated (Gazdar, Gao et al. 2010). Human bronchial epithelial cell lines with viral-mediated immortalization may therefore be more appropriate in studies of later stages of lung carcinogenesis. Recently, human bronchial epitheilial cells have been immortalized by the insertion of the telomerase (hTERT) catalytic subunit and the cyclin-dependent kinase 4 (CDK4) (Ramirez, Sheridan et al. 2004). These HBECs have an intact *p53* checkpoint and are genomically stable. They may therefore be considered a suitable model to study early premalignant changes in lung carcinogenesis.

An *In vitro* model may be helpful for the identification of premalignant molecular changes in order to acquire increased knowledge of early steps in lung carcinogenesis. Such models have been restricted by the immortalized cell lines available. An *in vitro* transformation model, using HBEC-KT cells, has recently been developed (Damiani, Yingling et al. 2008). HBECs do not form colonies in soft agar or tumors in nude mice at the starting point. In this model, cells that acquire the ability of anchorage independent growth, and thus form colonies in soft agar are defined as transformed. Transformed cell lines can then be used to investigate molecular changes associated with transformation.

1.10 Aim of the study

The aim of this study was to establish an *in vitro* transformation model for studies of molecular changes during premalignant transformation. Steroid receptor pathways have been hypothesized to be involved in carcinogen induced transformation. Because we have an interest in steroid receptor pathways in relation to carcinogen metabolism, this

in vitro transformation model would include exposure of HBECs to indirect-acting carcinogens, such as B[*a*]P, in order to test the cells capacity to bioactivate this carcinogen sufficiently for transformation. We also wanted to test other, including direct-acting, tobacco smoke carcinogens.

Further, if HBECs were transformed, the aim was to establish transformed cell lines to be used to investigate molecular and morphological changes resulting from bioactivation and carcinogen induced transformation. Transformed cell lines would be used to investigate if changes in gene expression among steroid receptor pathway members, including the *FOXA* genes, were associated with transformation. Also, both cellular and molecular changes associated with EMT would be investigated to determine if EMT could be involved in carcinogen induced transformation. Finally, epigenetic mechanisms are highly involved in carcinogenesis and also in the regulation of steroid receptor pathways and EMT. Therefore, we also wanted to test for epigenetic changes in transformed cell lines.

2 Materials and method

An *in vitro* transformation model of human lung epithelial cells was used to study early steps of chemically induced lung carcinogenesis. An overview of the cellular and molecular analysis that were performed during and after the transformation assay, are shown in Figure 2.1.

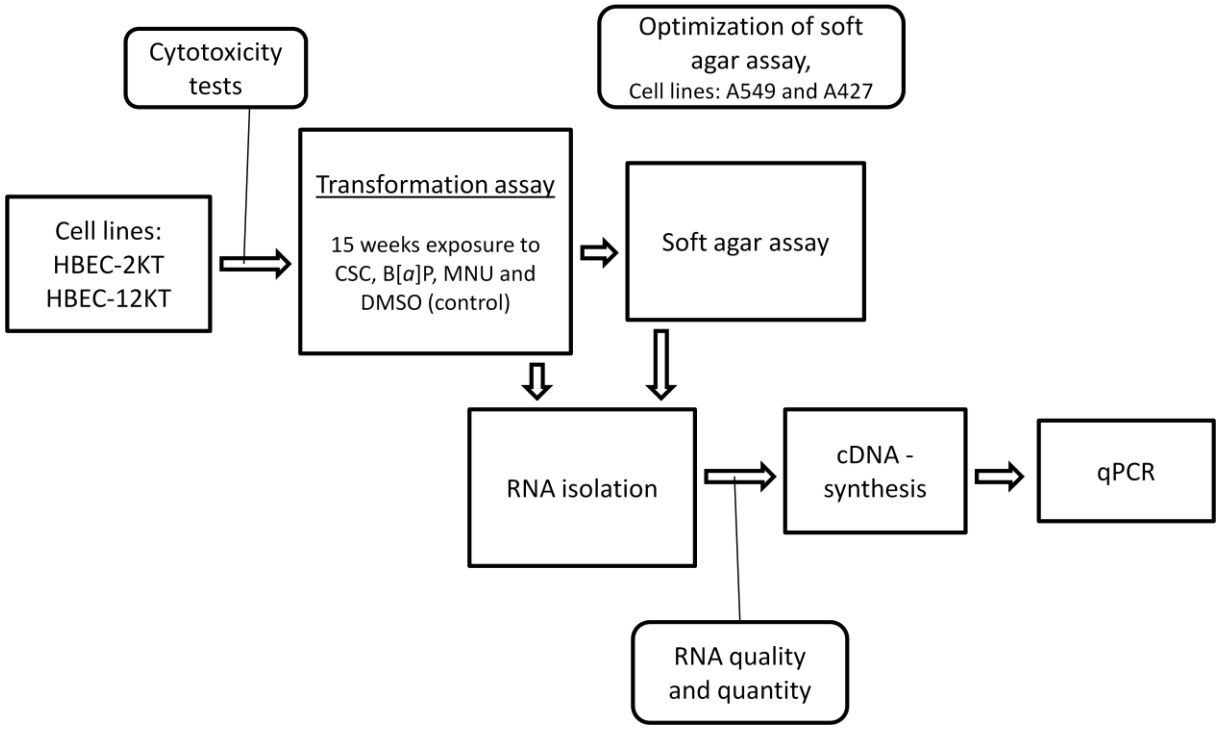

Figure 2.1: Outline of methods used.

2.1 General cell work and optimization.

All cell work was performed under sterile conditions in OAS LAF benches with gas burner, ventilation and with the use of plastic pipettes (Fisher Scientific). Protocols for general cell work, such as passaging of cells and freezing of cells for storage, are described in Appendix A. Cells were grown in 100 mm dishes, 96 well-, 6 well- or 24 well-plates (NUNC, Nunclon surface sterile) and passaged when 80 % confluent. The HBECs were grown on collagen coated dishes (see Appendix A).

2.1.1 Cell lines and culture conditions

Cells were taken up from STAMIs liquid nitrogen cell bank and cultured at 37 °C in a humidified 5 % CO_2 atmosphere (Thermo Forma incubator). hTERT/Cdk4-immortalized bronchial epithelial cells (HBEC) were used for the transformation assay. HBEC were grown in LHC-9 medium (Gibco, Invitrogen, cat.no. 12680-013) added 1% PS and 10%

FBS (see Appendix G). The characteristics of the three different HBEC cell lines that were available are outlined in Table 2.1. The tumor cell lines A549 and A427 were used for optimization of soft agar assay. A427 cells were grown in RPMI 1640 medium (Gibco, Invitrogen ref. 21875- 034) and A549 cells in DMEM/F-12 (Gibco, Invitrogen, ref: 21331-020) both added 1% PS and 10% FBS.

Table 2.1: Properties of the HBEC cell lines at STAMIs cell bank

Cell line	Age of donor	Sex of donor	Diagnosis
HBEC-2KT	68	Male	NSCLC
HBEC3-KT	65	female	No cancer
HBEC-12KT	55	female	NSCLC

2.1.2 Seeding of cells for experiments

The following is a description of the general procedure for seeding of cells for experiments. This procedure, including materials and reagents, will not be repeated for each experiment, specific details only. The volumes of the different solutions were adapted to the size of the dishes used. This description is for 100 mm dishes.

Materials	Reagents
Microcentrifuge tubes. 0.5 ml and 1.5 ml (Trefflab)	Suitable growth medium
Light microscope (Nikon Diaphoto)	DNAse , from bovine pancreas, 4 mg/ml (Sigma)
Centrifuge tubes (Falcon)	Trypsin , 0.05 % in PBS (Gibco, Invitrogen)
Cellteller, Countess-Automated Cell-Counter (Invitrogen)	Trypan blue stain 0.4% (Invitrogen)
Cell Counting chamber slides (Invitrogen)	
Centrifuge (Eppendorf 5702)	

Protocol

1. 80 % confluent cultures were the starting point for experiments. The medium over the cells was removed.
2. The dish was washed twice with 8 ml PBS.
3. 1 ml trypsin solution was added, and the cells were incubated at 37 °C until they had loosened from the dish, which was visible in the light microscope.
4. 5 ml growth medium was added the cell-suspension was transferred to a centrifugation tube and centrifuged for 4 minutes at 1000 rpm.
5. The supernatant was removed and the pellet was re-suspended in 5 ml growth medium. Certain cell lines (A427, A459) required the addition of 20µl DNAase to the pellet to obtain single-cell suspension.
6. Cells were counted using a Countess automated cell counter. 10 µl cell suspension was mixed with 10 µl trypan blue stain in a 0.5 ml microcentrifuge tube. 10 µl of this mix was then pipetted onto Cell Counting chamber slides.

7. The cell suspension was mixed with new growth medium to obtain the desired cell density. Countess automated cell-counter calculated this. Cells were seeded on 6 or 96-well plates.

2.1.3 Cytotoxicity test with CellTiter Blue assay

The reagent CellTiter-Blue (CTB) uses the indicator dye resazurin to measure the metabolic capacity of cells, an indicator of cell number or cell viability. Viable cells reduce resazurin into resorufin, which is highly fluorescent and emits fluorescence at 590 nm. The fluorescence produced is proportional to the number of viable cells. The CTB assay was used to test toxicity of B[*a*]P to HBEC cell lines. Different quantities of cells were seeded on a 96-well plate and fluorescence was measured to show this relationship (see Appendix B).

Materials	**Reagents**
Modulus microplate reader (Turner Biosystems)	B[*a*]p (Sigma B-1760-1G)
96-well plates (NUNC, Nunclon surface sterile)	99.99 % DMSO (Kock Licht 2228-00)
	CellTiter Blue-reagent, CTB (Promega)

Protocol

1. Day one, HBEC-2KT and HBEC-12KT were seeded out, 800 cells/well on 96-well plates, and incubated for 24 hours.
2. Day two, Cells were exposed to 0.33, 1, 3 and 10 µM B[*a*]P in LHC-9 medium. Solutions of 0.33, 1, 3 and 10 mM B[*a*]P were made in DMSO. These were diluted 1:1000 in LHC-9 medium, resulting in a final concentration of 0.1 % DMSO. Medium containing DMSO only was used as control.
3. Day four, the medium over the cells was removed and step 2 was repeated.

4. On day seven, the medium over the cells was removed. The cells were washed twice with PBS. CTB reagent was added to each well (15 µl CTB/100µl medium). CTB was also added to empty wells to make a blind control. The plates were then left for two hours at 37 °C in the cell incubator.
5. Fluorescence was measured at 560/590nm in the Modulus microplate reader.
6. Fluorescense of the blind control was subtracted from fluorescence of the cells.

2.1.4 Cytotoxicity test with Countess- Automated Cell-Counter

Countess- Automated Cell- Counter measures the number and fraction of live cells. This can be used to measure cytotoxicity. HBEC-2KT and 12-KT were exposed to B[*a*]P, CSC and DMSO. Several cell counting tests with B[*a*]P and CSC were performed and different protocols were used, including different exposure frequencies. Exposure duration varied from four hours until three days. The following is a description of the protocol for one week exposure.

Protocol

1. Day one, HBEC-2KT and HBEC-12KT were seeded, 10 000 cells/well on 6-well plates and incubated for 24 hours.
2. Day two, cells were exposed to 0.33, 1, 3 and 10 µM B[a]P in LHC-9 medium and 1.11, 3.33, 10 and 30 µg/ml CSC in LHC-9 medium. Both agent were diluted in DMSO (0,1 % final concentration) and DMSO only was used as a control.
3. Day four, the medium over the cells was removed and step 2 was repeated.
4. On day seven, the medium was removed and 1 ml trypsin was added. The plates were incubated until they had loosened from the dish, visible in light microscope.
5. Cells were counted using the automated cell counter. The number of live cells per well and the fraction live/dead was registered.

2.2 Transformation assay – 15 weeks chemical exposure

HBEC-2KT and HBEC-12KT were exposed to different tobacco chemicals weekly for 15 weeks. Each cell line was subjected to 6 different exposures weekly (see Table 2.2). Each exposure experiment was performed in 4 parallels.

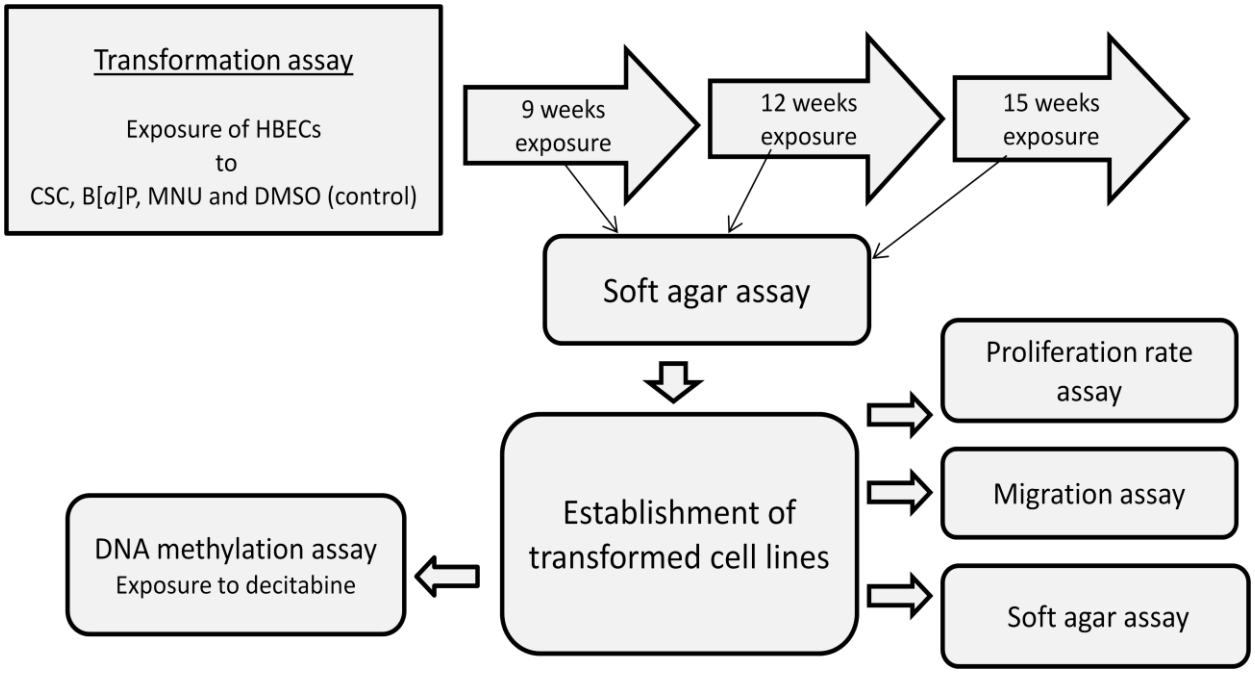

Figure 2.2: Outline of cellular assays performed during and after the transformation assay. All stages were inspected in the light microscope for morphological changes.

Table 2.2: Table shows the different carcinogen doses and exposure durations for each cell line.

	MNU	B[*a*]P	CSC	DMSO (Control)
HBEC-2KT	1 mM 1 hour	Low dose 0.33 µM , 3 days	Low dose 1 µg/ml, 3 days	0.1 % 3 days
		High dose 1 µM, 3 days	High dose 3 µg/ml, 3 days	
HBEC-12KT	0.5 mM 1 hour	Low dose 0.33 µM, 3 days	Low dose 1 µg/ml, 3 days	0.1 % 3 days
		High dose 1 µM, 3 days	High dose 3 µg/ml, 3 days	

At several stages during the exposure period, cells were taken out and seeded on new 6-well plates for various molecular analyses. After grown to confluence and washing three times in PBS, dishes for RNA analysis were put in -80°C freezer, while dishes for DNA and

protein analysis were put in the -20°C freezer until further processing (to be carried out in the lab after this master project)

Protocol

1. Day one, cells were seeded in 1.5 ml medium on 6-well plates and incubated for 24 hours. HBEC-2KT was seeded at 10 000 cells/well and HBEC-12KT at 20 000 cells/well.
7. Day two, exposures were initiated. Solutions of 0.33 and 1 mM B[*a*]P, 1 and 3 mg/ml CSC and 1 M MNU were made in DMSO. These were diluted 1:1000 in LHC-9 medium, resulting in a final concentration of 0.1 % DMSO. Medium containing DMSO only was used as control.
2. After one hour MNU was removed from the cells. The dishes were washed in PBS and 2 ml fresh LHC-9 medium/dish was added.
3. Day five, B[*a*]P and CSC was removed from the cells. The dishes were washed in PBS and 2 ml fresh medium was added. In addition, the medium over the MNU exposed cells was changed.
4. Day eight (day one in the next week), the cells were passaged, counted, and seeded on new 6-well plates (see 2.1.2) at cell densities described above.
5. The procedure was repeated for 15 weeks.

2.3 Soft agar assay

The soft agar assay is an *in vitro* cellular transformation detection assay. In this study, it was used to measure cell transformation induced by carcinogens. This transformation is associated with certain phenotypic changes, such as loss anchorage independence. Anchorage independence gives the cells an ability to form colonies in soft agar.

Anchorage independent growth, and thereby colony formation in soft agar, is a typical trait for tumor cell lines. To optimize the soft agar protocol, the human lung tumor cell lines A549 and A427, which have previously been shown to form colonies in soft agar, were used.

The soft agar is composed of a base-layer and a top-layer. The base-layer is made first. After solidifying, a top-layer containing a lower concentration of agar and a specified number of cells is added. Each of the parallels from the exposure regimen was seeded

out on two 6-well plates. While working, the agar solutions were kept in a water bath at 45 °C. It was important to work fast so that the agar solutions did not gel before they were supposed to. The agar was not mixed with cells before the temperature was under 37 °C.

For the HBEC-2KT and 12-KT cell lines, cells were taken out from the exposure regimen after 9, 12 and 15 week of chemical exposure and seeded in soft agar to test for transformation.

Protocol

1. 1 g Difco agar noble (BD, ref.214220) was mixed with 33.3 ml PBS to obtain a 3 % agar stock solution which heated on a warming plate until boiling.
2. This agar stock solution was autoclaved on the program for agar solutions (Systec DX-90).
3. The 3 % agar stock solution was mixed with growth medium to obtain 0.7 % base agar.
4. 1.5 ml 7 % base agar was added each well in 6-well plates and allowed to gel at 4 °C.
5. Cells were trypsinized and counted and the cell suspension was diluted in medium to obtain 2000 cells/ml.
6. This cell suspension was mixed with an equal volume 0.7 % agar solution to obtain 0.35 % top agar solution with 1000 cells/ml.
7. 1 ml of this cell-containing top-agar was added on top of a base-agar-containing well.
8. The plates were immediately put at 4 °C and kept there for 30 minutes to allow for the top-agar to gel. This was followed by incubation at 37 °C for at least 3 weeks.
9. 500 µL fresh medium was added after two days. This medium was changed once a week.

2.3.1 Crystal violet staining of cells and colony counting

Plates were inspected in the light microscope for appearance of colonies daily. To visualize and count colonies in soft agar, staining with Crystal violet was used. When

dissolved in water, Crystal violet has a blue violet color. Crystal violet stains cell walls, so that cell colonies will be clearly visible.

1. Crystal violet (Sigma) was dissolved in autoclaved water in two steps. First, to obtain a 0.1 % crystal violet solution, and then to obtain the final 0.005 % crystal violet solution.
2. 500 µl of this solution was added on top of the soft agar dishes and incubated for 30 minutes.
3. Colony formation was inspected in light microscope and photos were taken.

2.4 Establishment of transformed cell lines.

Cell colonies in soft agar were taken out and grown further in monolayer. These transformed cells were allowed to replicate for approximately 3 weeks to reach populations large enough for further analysis. They were seeded in soft agar a second time to make sure that the trait of anchorage independent growth was persistent, and that these cells from the colonies were truly clonal. In addition, transformed cells were seeded on new 6-well plates. After grown to confluence and washing tree times in PBS, these dishes for RNA analysis were put in -80°C freezer until further processing. Cells were also kept for storage at STAMIs liquid nitrogen cell bank for later use.

Protocol

1. Colonies were carefully isolated from the soft agar using a 200 µl pipette, while looking in the light microscope.
2. A single colony was mixed with 200 µl fresh medium in a 0.5 ml microcentrifuge tube, pipetted up and down to release the cells from soft agar and then seeded on 24-well plate. One colony was seeded in each well. Five to ten colonies were taken out from each cell line/exposure.
3. The plate was left in the incubator at 37 °C to allow the cells from the individual colonies to fasten and start growing.
4. After approximately two weeks (when the cell layers in these wells were confluent) the cells were passaged and seeded on 6-well plates.
5. After approximately one week these wells became confluent, the cells were passaged, and seeded on 100 mm dishes.

6. When the individual populations were large enough, cells were seeded in soft agar a second time. Cells were also seeded on new 6-well plates. After grown to confluence and washing three times in PBS, these dishes for RNA analysis were put in -80 °C freezer until further processing.

2.5 Proliferation assay

Proliferation rates were determined during the exposure period and on a subset of the transformed cell lines.

Protocol

1. Cells were seeded on 6-well plates, 20 000 cells/well (HBEC-12KT), and 10 000 cells/well (HBEC-2KT) in 4 parallels.
2. After four days, they were counted, using the Countess- Automated Cell- Counter (see 2.1.2)
3. Proliferation rates were calculated using the following formula:

$-(\log c)\cdot(\log n)/3(\text{days})\cdot\log 2 = \text{Cell divisions/day}$

c = number of cells counted the final day. *n* = number of cells seeded out.

("Working with bacterial yields and growth rates", available at: http://www.mgm.ufl.edu/~gulig/bacgen/handouts/growth.PDF, accessed at 30.05.12)

2.6 Migration assay

Increased cellular motility and migration capability is a characteristic associated with EMT. In this migration assay, confluent dishes were scraped with a metal spatel to make an "open wound" in the cell monolayer. The cells ability to migrate into the open wound was then monitored.

Protocol

1. Transformed cell lines and non-transformed control were seeded on 100 mm dishes at a high density (500 000 cells/well) to obtain confluent dishes.
2. The next day, a metal spatel was used to create a scratch in the cell monolayer. This was done carefully to avoid scratching the plate and thereby making migration barriers.

3. A spot along this line was marked, and the plates were frequently observed in the light microscope and photographed at defined time intervals.

2.7 DNA methylation assay

The nucleotide analog decitabine (5-Aza-2`-deoxycytidin) can be used to remove DNA methylation. By removing DNA methylation it is possible to get indications whether observed gene expression changes are caused by silencing through DNA methylation. Decitabine, which cannot be methylated, removes DNA-methylation by its incorporation in DNA under replication. It also binds to DNMTs and inhibit their activity. As a result, DNA methylation levels will be significantly reduced after a couple of replications with the reagent present. Gene expression analysis performed on cells treated with decitibine can be compared with gene expression on untreated cells and changes may be indicative of DNA methylation.

Protocol

1. Day one, transformed cells were seeded on two 6-well plate, 500 000 cells/well.
2. Day two, cells were exposed to 100, 200 and 500 nM decitabine and DMSO in three parallels.
3. After one week of exposure, cells were washed three times in PBS and stored in the -80 °C freezer until RNA isolation.

2.8 Molecular analysis

Several molecular analyses were performed on the established transformed cell lines (Fig 2.3).

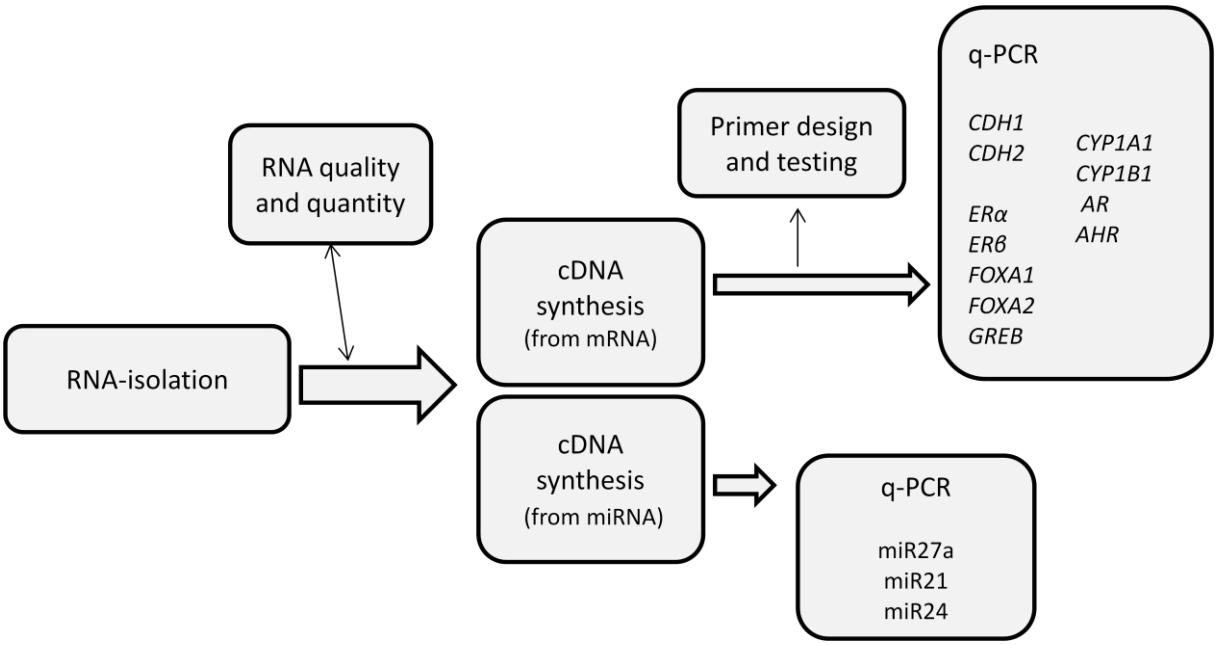

Figure 2.3 Outline of molecular analysis.

2.9 RNA-isolation

Cells for RNA isolation were taken out from the -80°C freezer. RNA was isolated using Isol-RNA Reagent. This is a monophasic solution of phenol and guanidine thiocyanate that disrupts and homogenise cells and tissues. It also inhibits RNAses. Isol-RNA isolates total RNA and this method is suitable for further analysis of both mRNA and miRNA. When chloroform is added to the Isol-RNA homogenate and the solution is centrifuged, there will be a separation into three phases: the aqueous (upper) phase that contains RNA, the interphase that contains DNA, and the organic (lower) phase that contains proteins. RNA is precipitated with isopropanol.

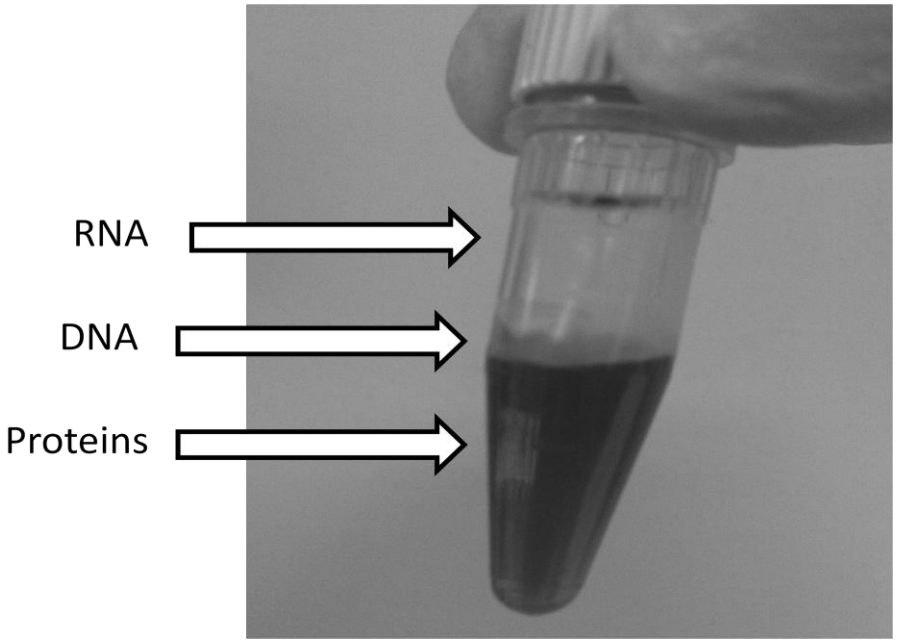

Figure 2.4: The separation in three different phases after step 4 in RNA isolation the protocol below.

Materials:	**Reagents:**
Twist top vials, with cap (Sorensen Bioscience, Inc)	Isol-RNA (5-prime, kat. No. 2302700)
Centrifuge (Eppendorf Centrifuge 5417R)	Chloroform (Sigma-aldrich)
Heating block (Grant QBT2)	Isopropanol (Merck)
Vortex (Heidolphreax 2000)	75 % ethanol (Kemetyl)
	DEPC-water (see Appendix G)

Protocol:

1. The 6-well plates were taken from the freezer and placed on ice. Isol-RNA Lysis Reagent (1 ml/35 mm well) was added.

2. A cell scraper was he used to loosen the cells from the plate. The lysate from each well was transferred to a twist top vial and incubated in room temperature for five minutes.
3. 0.2 ml chloroform was added to each vial which was incubated in room temperature for 2 to 3 minutes.
4. The vials where centrifuged at 12000 g, 4 °C, for 15 minutes.
5. The upper aqueous phase was transferred to a new twist top vial. It was important to avoid the contamination from the interphase. 0.5 ml isopropanol was added to each vial which was incubated at room temperature for 10 minutes.
6. The vials where centrifuged at 12000 g, 4 °C, for 15 minutes.
7. The supernatant was removed and discarded.
8. The pellets were washed with 1 ml 75 % ethanol and vortexed.
9. The vials were centrifuged at 12 000 g, 4 °C, for 15 minutes.
10. The supernatant was discarded and the pellets were dried for 15 to 20 minutes.
11. Each pellet was re-suspended in 10 ul nuclease free water and put on ice.
12. The vials were incubated at 65 °C for 10 minutes, spun down, mixed, and put on ice.
13. The vials were put in the -80 °C freezer for minimum one night.
14. The RNA samples were incubated at 65 °C for 10 minutes.
15. RNA was stored in the -80 °C freezer.

2.9.1 RNA quality and -quantity

Knowing the concentration of RNA is important to obtain correct dilution (1 ug/uL) that should be used in cDNA synthesis. An Eppendorf Biophotometer was used to determine nucleic acid quantity and quality. Nucleic acids have absorption maximum at 260 nm. RNA concentration was determined by measuring OD (260/280). A A260 absorption of 1.0 is equivalent to 40.0 ug/ml RNA (and 50.0 µg/ml dsDNA). The optimal value for this instrument lies between 0.1 and 1.

Pure RNA has a 260/280 ratio of 2.0, while pure DNA has a ratio of approximately 1.8. A lower ratio may indicate contamination by proteins (aromatic groups) or phenol. Aromatic groups have an absorption maximum at 280 nm, while phenols have

absorption maximum at 270 nm. Carbohydrates have absorption maximum at 230 nm. A 260/230 ratio lower than 2.0 indicates possible contamination of sugar, salt or organic solutions.

Materials	Reagents
Biophotometer (Eppendorf)	TE-buffer (see Appendix G)
Quarts cuvettes (QS-Hellma)	DEPC water (see Appendix G)
0.5 ml microcentrifuge tubes (Trefflab)	

Protocol

1. 1 µL RNA sample was mixed with 69 µL TE-buffer in 0.5 ml microcentrifuge tubes to obtain a 70x dilution of each sample.
2. Samples were then transferred to quarts cuvettes. RNA concentration was determined by using the biophotometer at 260 nm and 280 nm.

After the measurements, the samples were diluted, if large enough quantities, to obtain 1 ug/uL for cDNA synthesis. The samples were stored at -80 °C, until further use.

2.9.2 RNA quality

RNA quality was measured on a subset of RNA samples by using Agilent Bioanalyzer RNA 6000 Nano Kit (No. 5067-1511). Method and results are described in the Appendix C.

2.10 cDNA Synthesis of mRNA

Complementary DNA (cDNA) was synthesized from mRNA using the qScript cDNA Synthesis Kit (Quanta BioSciences). This kit contains an optimized blend of random and oligo(dT) primers. They provide, together with the polyA-tail, a double-stranded sequence at the 3' end of the mRNA. cDNA is then synthesized from RNA by reverse transcriptase (RT) enzyme.

Materials	Reagents
Perkin Elmer Cetus DNA Thermal Cycler 480	qScript cDNA Synthesis kit (Quanta BioSciences)
0.5 ml microcentrifuge-tubes (Trefflab)	TE-buffer (see Appendix G)
Vortex (Heidolpreax 2000)	
Heating block (Grant QBT2)	

Protocol

1. Microcentrifuge tubes were marked with sample name and date.
2. RNA samples (1 ug/ml) were taken out from -80 °C freezer, put on ice, and thawed on a heating block at 65 °C.
3. A master mix was made and mixed with RNA samples in the pre-marked microcentrifuge tubes as described in Table 2.3.
4. The microcentrifuge tubes were incubated in the thermal cycler at the program described in table 2.4.
5. 80 µL TE-buffer was then added each sample. The cDNA was stored at -20 °C.

Table 2.3: Volume/sample of the reagents for cDNA synthesis.

Reagents	Volume/sample (uL)
DEPC- water	14
RNA template (1ug/uL)	1
qScript cDNA supermix	4
qScript RT-enzyme	1
Total volume	**20**

Table 2.4: Thermal cycle program for cDNA synthesis

Program step:	Temperature, °C:	Time, minutes:
Incubation (primer annealing)	22	5
cDNA synthesis	42	60
Incubation (denaturing of enzymes)	85	5
Cooling	4	5

2.11 cDNA synthesis from miRNA

For cDNA synthesis from miRNAs, qScript microRNA cDNA Synthesis Kit (Quanta BioSciences) was used. MicroRNAs are not polyadenylated in nature, and consequently oligo-dT primers cannot be used directly for cDNA synthesis as in cDNA synthesis of mRNA. Therefore, miRNA is polyadenylated in a poly(A) polymerase reaction. qScript Reverse Transcriptase and other necessary reagents are subsequently added to convert the poly(A) tailed miRNAs into cDNA using an oligo-dT adapter primer.

Protocol

Poly(A) Tailing Reaction

1. Microcentrifuge tubes were marked with sample name and date.
2. RNA samples (1 ug/ml) were taken out from -80 °C freezer, put on ice, and thawed on the heating block at 65 °C.
3. The following necessary components were added to the premarked microcentrifuge tubes, which were then vortexed and centrifuged (see Table 2.5)
4. The tubes were incubated for 60 minutes at 37 °C followed by 5 minutes at 70 °C in the Perkin Elmer Cetus DNA Thermal Cycler 480.

Table 2.5: Volume of reagents for each sample for Poly(A) tailing reaction.

Reagents	Volume/sample (ul)
DEPC water	variable
RNA template (up to 1 ug RNA)	Up to 7
Poly(A) Tailing buffer	2
Poly(A) polymerase	1
Total volume	**10**

First strand cDNA Synthesis Reaction

5. Components were mixed in new microcentrifuge tubes as described in Table 2.6, vortexed and centrifuged.
6. The tubes were incubated 20 minutes at 42 °C followed by 5 minutes at 85 °C.
7. 80 µL TE-buffer (see Appendix G) was then added each sample. The miRNA cDNA was stored at -20 °C.

Table 2.6: Volume of reagents for each sample for First strand cDNA Synthesis Reaction.

Reagents	Volume/sample (uL)
Poly(a) Tailing reaction (from step 4 above)	10
microRNA cDNA Reaction mix	9
qScript Reverse Transcriptase	1
Total volume	**20**

2.12 Quantitative real-time PCR (qPCR)

The polymerase chain reaction (PCR) is a method for amplification of DNA sequences using repeated cycles of altering high and low temperatures. Real-time PCR (qPCR) is a variant of traditional PCR, and is a much used method for examining gene expression. qPCR uses a fluorescent reporter molecule that binds the PCR product and reports its presence by fluorescence. In the work for this thesis the fluorescent reporter SYBR green was used. As the amount of product increases exponentially during the PCR, the

fluorescent signal also increases exponentially, reflecting the amount of product produced. Product detection is performed in the exponential phase. A doubling of DNA molecules is presumed for each amplification cycle. Based on this, the instrument can calculate the concentration of DNA template at the beginning, by using a threshold value (*Cq* value).

Melting curve analysis

Melting curve analysis was performed at the end of each qPCR to control for specificity of the reaction. Primer dimers and hairpin structures will result in shorter PCR products, which will show lower melting temperatures.

Temperature cycle program

The PCR reaction consists of a series of repeated temperature cycles. For the work in this thesis an initial activation and denaturing step at 95 °C for two minutes was used. At this step the DNA polymerase was activated, and DNA became single-stranded. The next step was 40 cycles with denaturation of cDNA at 95 °C for 10 seconds followed by a primer annealing and extension phase at 60 °C for 30 seconds. The newly synthesized DNA strand was template in the next amplification cycle. After 40 cycles one would theoretically have $X \cdot 2^{40}$ copies if X was the number of copies at starting points and a doubling at each cycle was assumed.

Reference gene

To compare different samples, it is necessary to have a reference (or normalization) gene. This is important because there might be a variation in the quality of cDNA synthesized from different samples. This might be due to variation in degradation of the RNA samples and to the efficiency of the cDNA synthesis. By including a reference gene, this can be compensated for. For the work in this thesis *β-actin* was used as a reference gene. This gene is highly and relatively stably expressed and has turned out to be largely unaffected by the different experimental conditions showed here.

Standard curve

A standard curve was made as a 4 x dilution series of a mix of samples. Such a dilution gives rise to a theoretically *Ct* distance of two cycles between each dilution. It was important that in each PCR cycle, there was a (close to) doubling of product, and that

the two cDNA dilution curves were parallel. The gene expression for *β-actin* between the different experiments was examined for eventual biological variation.

One standard curve was created for each gene in the experiment. In case of a 100 % effective PCR reaction the slope of the standard curve will be -3.33. Values between -3.1 and -3.6 were also accepted as long as the standard curves were parallel because this means that the normalization of gene and target gene had similar efficiency.

2.13 mRNA qPCR

qPCR of cDNA from mRNA was performed by using two primers in opposite directions of the desired gene. The primers were designed to span one or more introns, such that amplification of genomic DNA residues in the cDNA sample was avoided.

*C*t values between 20-30 cycles were considered to be optimal for all genes and the cDNA samples were accordingly. *β-actin* is highly expressed, and therefore a cDNA amount equivalent to 5 ng RNA input in the cDNA synthesis was used in the qPCR reactions. The amount of *CYP1A1, CYP1B1, AR, AHR, ERβ* and *ERα* was 100 ng since these genes has low expression.

Concentration of all primers was 25 pmol/µl. For mRNA qPCR PerfeCTa SYBR Green FastMix, ROX (Quanta Biosciences) was used. This kit contains AccuFast Taq DNA polymerase, SYBR Green I dye, ROX as an internal fluorescence reference, along with buffer and stabilizers.

2.13.1 Primer design and testing

Primers for *FOXA1, FOXA2, GREB, CDH1* and *CDH2* were designed by using the NCBI primer BLAST. The primers should optimally have a GC-content between the 40-60 % and the amplicon should be between 50-150 bases.

Table 2.7: Primer sequences for genes that were used in this thesis.

Gene	Primer sequence 5`→3`	Reference:
GREB	**Forward:** 5`-CAAAGAATAACCTGTTGGCCCTGC-3` **Reverse:** 5`-GACATGCCTGCGCTCTCATACTTA-3`	Designed for this thesis: http://www.ncbi.nlm.nih.gov/tools/primer-blast/
FOXA1	**Forward:** 5`-GGGGGTTTGTCTGGCATAGC-3` **Reverse:** 5`-GCACTGGGGGAAAGGTTGTG-3`	Designed for this thesis.
FOXA2	**Forward:** 5`-GGAGCAGCTACTATGCAGAGCC-3` **Reverse:** 5`-TGTTCATGCCGTTCATCCCCA-3`	Designed for this thesis.
CDH1	**Forward:** 5`-ACGCCGAGAGCTACACGTTCA-3` **Reverse:** 5`-TCCTTTGTCGACCGGTGCAATC-3`	Designed for this thesis.
CDH2	**Forward:**5`-TCCAACGGGGACTGCACAGAT-3` **Reverse:** 5`-GGCGTTCTTTATCCCGGCGTT-3`	Designed for this thesis.
B-actin	**Forward:** 5`-GCGAGAAGATGACCCAG-3` **Reverse:** 5`-GATAGCACAGCCTGGATA-3`	(Mollerup, Berge et al. 2006)
CYP1A1	**Forward:** 5`-CATCCCCCACAGCACAACA-3` **Reverse:** 5`-CAGGGGTAGGAAACCGTTCA-3`	(Mollerup, Berge et al. 2006)
CYP1B1	**Forward:** 5`-CTGGATTTGGAGAACATACCG-3` **Reverse:** 5`-TGATCCAATTCTGCCTGCAC-3`	(Mollerup, Berge et al. 2006)
AHR	**Forward:** 5`-CCCTTGGAAAATCATTGCCA-3` **Reverse:** 5`-GGAGAGGTGCTTCATATGTCGTC-3`	(Mollerup, Berge et al. 2006)
ERα	**Forward:** 5`-ACTTGCTCTTGGACAGGAACCA-3' **Reverse:** 5`-CAAACTCCTCTCCCTGCAGATT-3'	Designed for this thesis.
ERβ	**Forward:** 5`-GCCGACAAGGAGTTGGTACAC-3' **Reverse:** 5`AACAGGCTGAGCTCCACAAAG-3`	Designed for this thesis.
AR	**Forward:** 5'-CCTGGCTTCCGCAACTTACAC-3' **Reverse:** 5'-GGACTTGTGCATGCGGTACTCA-3'	Designed for this thesis.

Primers for *FOXA1, FOXA2, GREB, CDH1* and *CDH2* were tested before gene expression analysis was performed. Standard curves were made for each gene. In addition to test if the primers would result in optimal PCR slope (slope close to -3.33) these standard curves will also give an idea of the expression levels of the genes, and then also how much cDNA to use for qPCR. Agarose Gel electrophoresis were performed to that the RT-qPCR products from primer testing. This was performed to make sure that it was only on products, and that the product had correct length (See Appendix D).

Protocol

1. The primers stock solutions were diluted (25 pmol/uL).
2. Water was filtered sterile through a sterile filter with a 10 ml syringe.
3. A mastermix was made for each gene, containing primers, PerfeCTa Syber Green Fastmix, and sterile-filtered dH_2O.
4. A 4x dilution of series was made to generate a standard curve. 100 ng was the starting point for each series.
5. 36 uL mastermix was added to PCR tube strips and 10 µL of each of the steps in dilution series was added this.
6. All steps were run in 2 paralells of 20 µL reaction on a 96-well PCR plate.
7. The 96 well plates were covered by a plastic film.
8. The PCR plate was centrifugated at 3000 rpm for 30 seconds.
9. The qPCR file was opened. The PCR plate was put into the machine and the program was started.

2.13.2 mRNA qPCR

mRNA RT-qPCR was setup by using a pipetting robot. qPCR was performed in 384 well plates with reaction volumes of 12 uL.

Materials	Reagents
Microcentrifuge tubes 0.5 ml and 1,5 ml (Trefflab)	PerfeCTa Syber Green Fastmix Primers
10 ml one time syringe (B. Braun Inject)	
Sterile filter (Pall Corporation, Acrodisc Syringe filters)	
25 ml centrifuge tubes	
384 wells plate (MicroAmp, Applied biosystems)	
Centrifuge (Sigma)	
Plastic film for 96-wells plate (MicroAmp, Applied biosystems)	
Real-Time RT-PCR instrument (ABI Prism 7900 HT)	
Multichannel pipette (micronic systems)	
SDS 2.2 Software (Applied biosystems)	

Protocol

1. The pipetting robot (Eppendorf EPmotion 5070) was used to setup qPCR of mRNA on 384 well plates. The robot program was made beforehand.
2. cDNA was pipetted onto a 96 well plate and put into the robot.
3. A master mix with all contents, except cDNA, was made for each gene in a 1,5 Eppendorf tube and put into appropriate location in the robot
4. Water was sterile-filtered and added into the appropriate well in the robot.

Table 2.8: Final volumes for each sample in mRNA qPCR.

Reagents	Volume/sample µl (96 well-plate)	Volume/sample µl (384 well-plate)
cDNA	10	10
dH_2O	12,08	1,5
PerfeCTa Syber Green Fastmix	23 uL	12
Primer forward, 25 pmol/uL	0,46 uL	0,24
Primer reverse, 25 pmol/uL	0,46 uL	0,24
Volume in mastermix:	26	14
Final volume/sample	36 uL	24
Reaction volume	18	12

2.13.3 miRNA qPCR.

qPCR detection of miRNAs was performed by using Perferta Universal PCR Primer (Quanta Biosciences). This primer is complementary to the adapter sequence added in the cDNA synthesis step. The other primer is miRNA specific (this is normally the entire mature miRNA sequence)

Protocol

1. The pipetting robot (Eppendorf EPmotion 5070) was used to setup qPCR of miRNA on 384 well plates. The robot program was made beforehand.
2. cDNA from miRNA was pipetted onto a 96 well plate and put into the robot.
3. A master mix with all contents except cDNA was made for each gene in a 1,5 eppendorf-tube and put into appropriate location in the robot (see table 2.9).
4. Water was sterile- filtered and added into the appropriate well in the robot.

Table 2.9: Final volumes for each sample in miRNA qPCR.

Component	Volume/sample
SYBR Green Supermix	12.02
Perferta microRNA Assay Primer (10 µM)	0.48
Perferta Universal PCR Primer (10 µM)	0.48
MicroRNA cDNA	10
DEPC water	1.02
Total volume	24

2.14 Statistical methods

Statistical analysis was performed by using GrapgPad InStat 3.0 Software (San Diego California, USA) $p<0.05$ was accepted as statistically significant. Comparison of multiple groups was performed by using one-way ANOVA followed by post hoc Tukey test.

3 Results

The result section has been divided into two parts. The first part contains results from the *in vitro* transformation of human bronchial epithelial cells. Cellular changes, such anchorage independent growth, morphological changes and results from the migration assay are described here. Part two describes results from gene expression analysis, miRNA expression and results from DNA methylation assay.

3.1 Optimization of carcinogen dose and exposure frequency.

In this *in vitro* transformation assay, it was the intention to mimic the situation occurring in the bronchial epithelium of the smoker, as close as possible. This was achieved by long-term exposure to tobacco smoke carcinogens. An important step in the optimization of this experiment was therefore to establish doses, as well as exposure frequencies and duration of the tobacco smoke carcinogens. Several cytotoxicity tests were performed for this purpose. The carcinogen dose should be as high as possible in order to provoke cellular changes, but low enough to not be cytotoxic. A cytotoxic dose was defined as one leading to more than 30 % reduction in viability. The cytotoxicity tests were performed by exposing HBEC cell lines to different doses of tobacco smoke carcinogen to establish the dose-response relationships.

The carcinogens chosen were B[*a*]P, CSC and MNU. Dose and exposure frequency of MNU was based on earlier similar experiments (Damiani, Yingling et al. 2008), and cytotoxicity tests were only performed with B[*a*]P and CSC. In addition, cytotoxicity test with medium added serum (FBS) were also performed to investigate if serum itself could influence cell behavior.

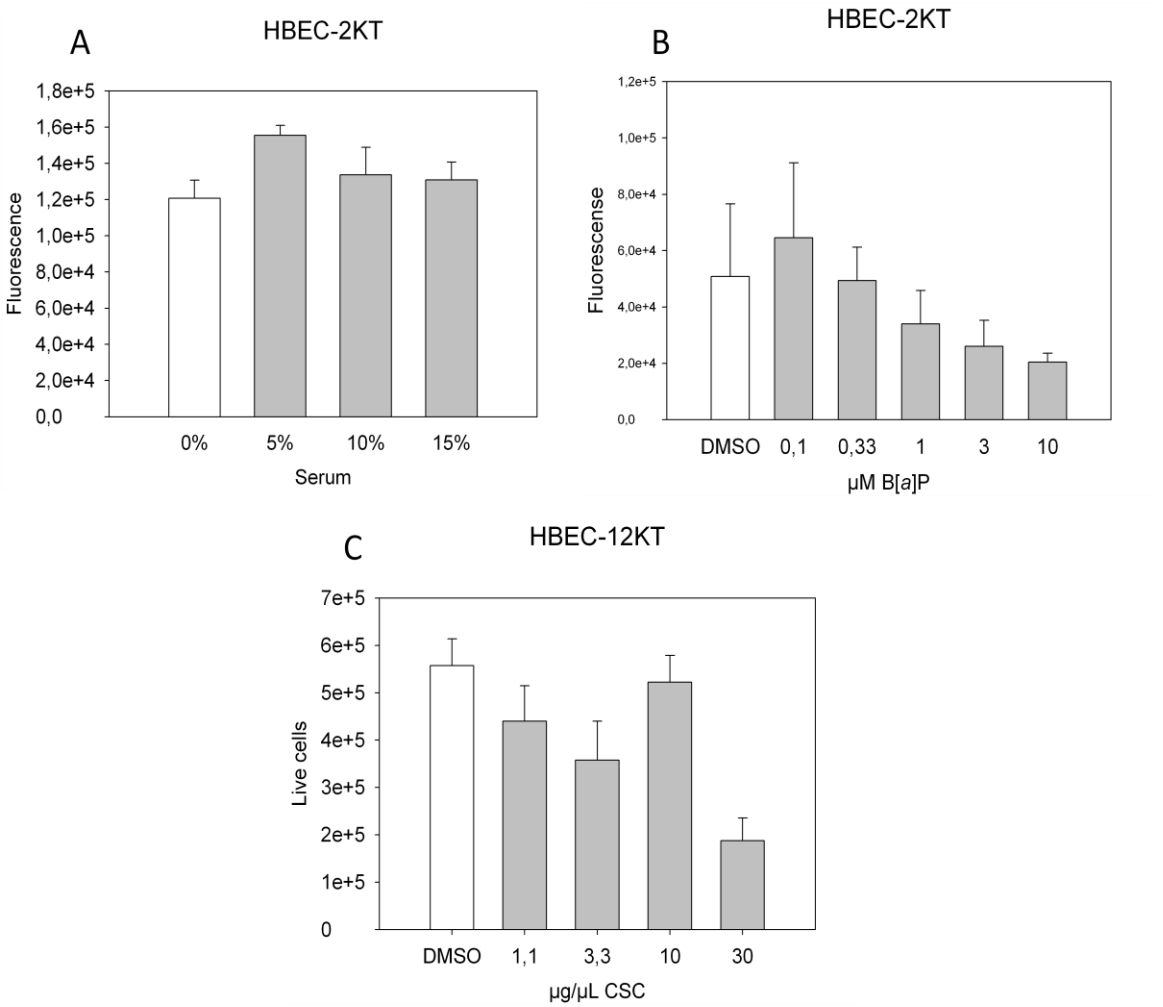

Figure 3.1: Different cytotoxicity test. Columns show the mean value SD. A) Serum toxicity tests performed with CTB, B) B[*a*]P cytotoxicity test performed with CTB and C) CSC cytotoxicity test performed with Countess Automated CellCounter. No statistical analyses were performed on these results because they were only optimization experiments.

Figure 3.1 shows the results of a subset of the tests performed. Several optimization tests were performed (not shown). Based on these and the results presented in Figure 3.1, two doses of B[*a*]P and CSC were chosen to use in the transformation assay. One low dose that almost did not show any toxicity at all: 0.33 µM B[*a*]P and 1 µg/ml CSC, and one high dose that resulted in approximately 20 % reduction in viability in repeated tests: 1 µM B[a]P and 3 µg/ml CSC. Different exposure durations, exposure frequencies and cell densities were also tested in these optimization tests. To avoid any cumulative toxicity in the 15 weeks transformation assay, exposure for 3 days once a week was chosen. Because the effect of carcinogens seemed to be affected by cell density as well as dose, it was important that the cell density was not too high. Optimal cell density should result in 80 % confluent dishes at the end of the week. Optimal cell density for

HBEC-2KT turned out to be 1000 cells/well, while for HBEC-12KT it turned out to be 2000 cells/well because of different sizes and proliferation rates of the cells.

All of the three available HBEC cell lines were used in these optimization experiments. Earlier results from transformation experiments with HBEC from a donor without lung cancer did not result in transformation after exposure to BPDE. Considering the fact that the unactivated carcinogen B[*a*]P was chosen for this experiment, and that this might have rendered the cells more refractory to transformation, the two cell lines from donors with NSCLC - HBEC-12KT from a female and HBEC-2KT from a male donor- were chosen.

3.2 Transformation

Before the long-term exposures were initiated in the transformation experiments, it was important to have an optimized soft agar assay ready. For the optimization of the soft agar assay, two tumor cell lines that have previously been shown to form colonies in soft agar were used. The soft agar assay contains a base layer and a cell-containing top layer. In the top layer it was important to have an agar concentration as low as possible, but still high enough for the agar to gel. The agar was solid in temperatures under approximately 35 °C so it was important to work quickly with the agar before it was solidifying. As long as the agar was not mixed with the cells, it was kept in water bath at 40 °C, but when this agar was mixed with cells it should not have a temperature above 37 °C. Several optimization experiments were performed and as Figure 3.2 shows the tumor cell lines A549 formed colonies in soft agar.

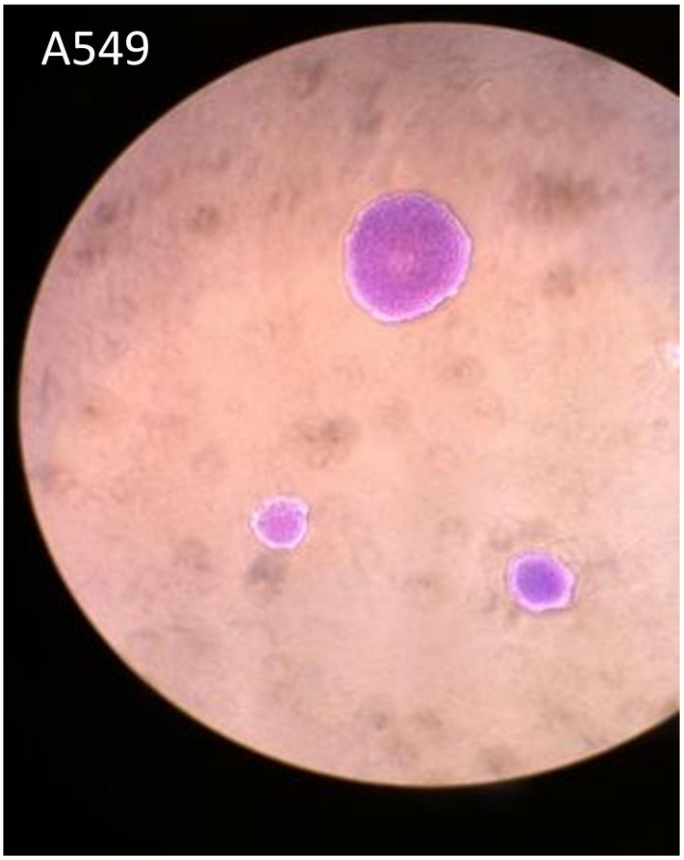

Figure 3.2: A549 colonies in soft agar and stained with crystal violet.

In the transformation assay, the two HBEC cell lines were exposed weekly for the 6 different treatments, including DMSO control. Colony formation in soft agar was tested after 9, 12 and 15 weeks of treatment. Cells that acquired the ability of anchorage independent growth and thereby formed colonies in soft agar were defined as transformed. All treatments were carried out in four parallels that were kept separated during the exposure time and these were seeded separately in soft agar. The number of parallels that formed colonies for each treatment may be indicative of transformation efficiency.

HBEC-2KT cells exposed to CSC formed colonies in soft agar after 9, 12 and 15 weeks exposure. Both doses of CSC and all of the four parallels of each dose resulted in colonies. HBEC-2KT cells exposed to B[*a*]P, MNU and DMSO were also seeded in soft agar, but none of these treatments resulted in colony formation. Figure 3.3 shows HBEC-2KT cells exposed to 1 ug/ml CSC for 12 weeks, after 3 weeks in soft agar.

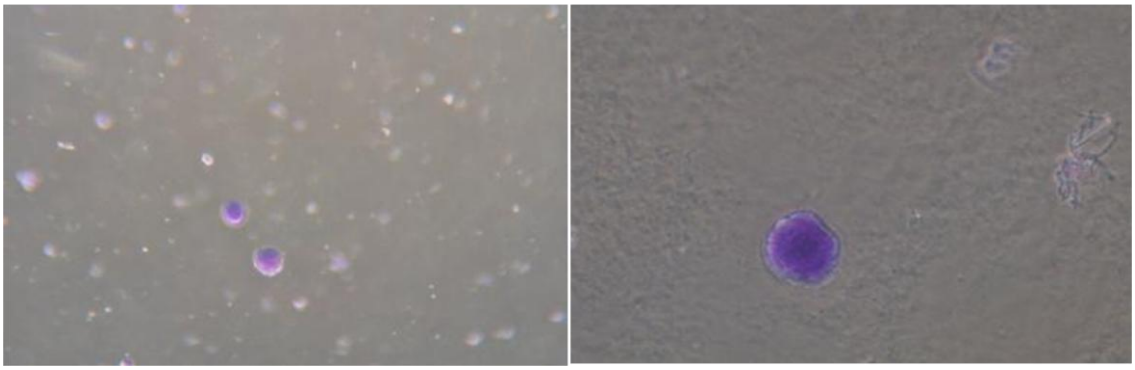

Figure 3.3: HBEC-2KT colonies after 3 weeks in soft agar and staining with crystal violet. Before seeding in soft agar, these cells were exposed to 1 ug/ml CSC for 12 weeks.

HBEC-12KT exposed to CSC, B[*a*]P and MNU formed colonies in soft agar (Fig. 3.3). Transformation efficiency differed among these carcinogens. Only one parallel of each dose B[*a*]P after 9 and 12 weeks formed colonies, and two parallels of each dose after 15 weeks. After 9 weeks only two parallels of the low dose of CSC formed colonies. Both doses of CSC formed colonies after 12 and 15 weeks (3 parallels). Three parallels of HBEC-12KT exposed to MNU formed colonies after 9 and 12 weeks, and surprisingly, this number was reduced to two after 15 weeks exposure. Exposure to DMSO for 9, 12 and 15 weeks did not, as expected, result in colony formation.

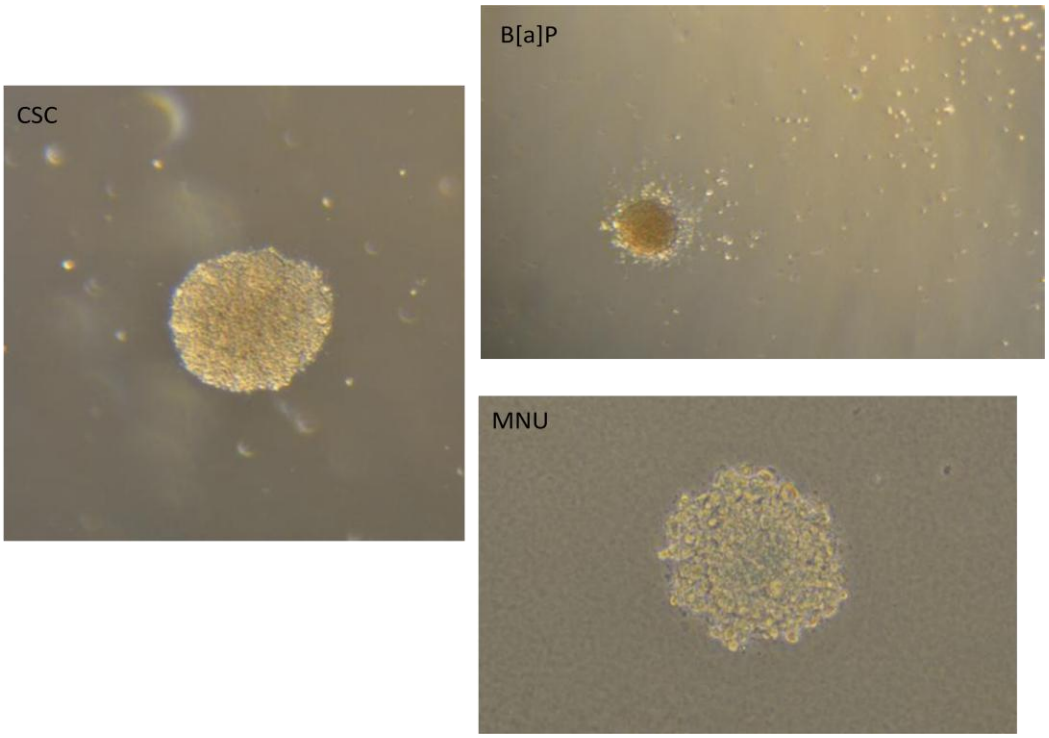

Figure 3.4: HBEC-12KT colonies after exposure to 1 ug/ml CSC, 0.33 uM B[*a*]P and 1mM MNU. These cells were not stained with crystal violet.

Figure 3.5 summarizes the results from the transformation and soft agar assays. Treatments that lead to colony formation are shown. Exposure to CSC had highest transformation efficiency since these exposures lead to transformation in both cell lines, while B[*a*]P exposure showed lowest transformation efficiency with only one, or a few parallels, in one cell line, growing as colonies.

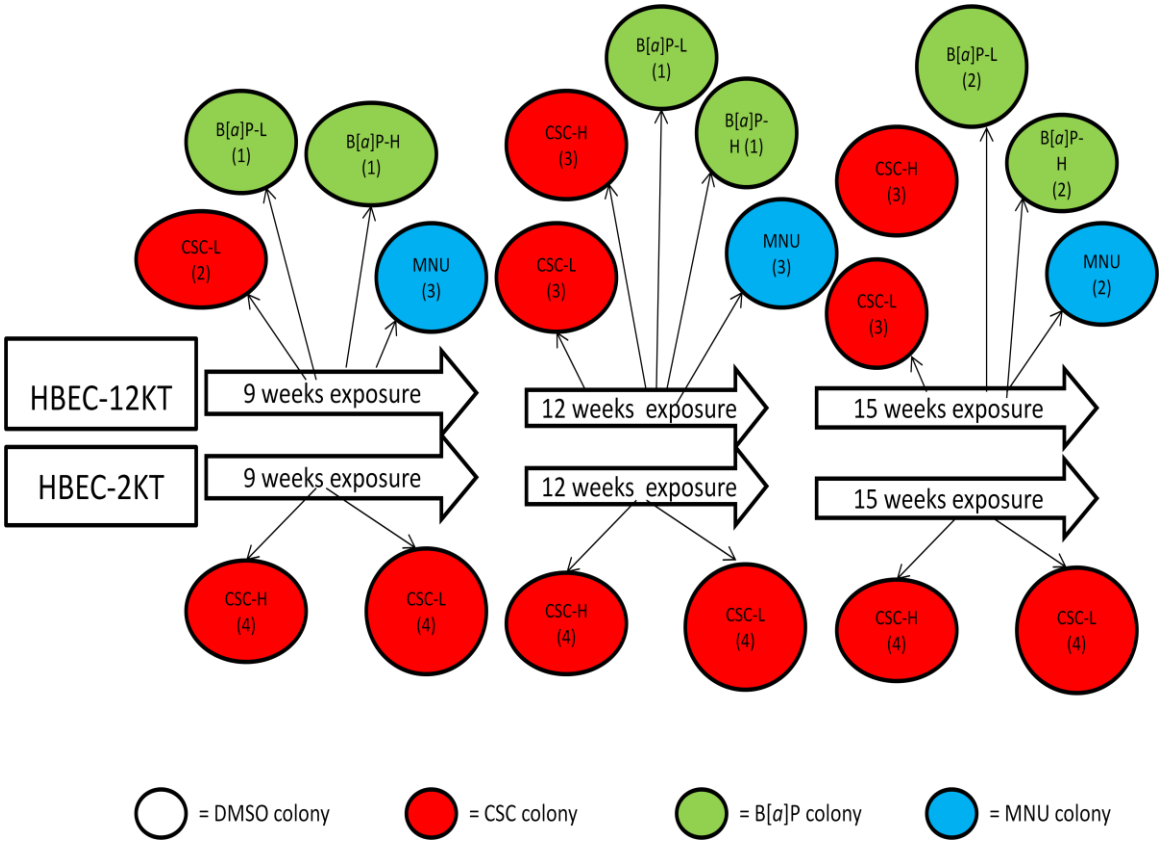

Figure 3.5: Treatments that resulted in colony formation in soft agar after 9, 12 and 15 weeks are illustrated. Type of carcinogen and the dose is also described: B[*a*]P –L = 0.33uM B[a]P , B[*a*]P-H = 1 uM B[*a*]P, CSC-L= 1ug/ml CSC, and CSC-H = 3 ug/ml CSC. The number of the parallels that resulted in colonies is written in parenthesis.

3.3 Establishment of transformed cell lines

Several treatments resulted in colonies after 9, 12 and 15 weeks (as previously shown). For the establishment of transformed cell lines that could be used in further analyses, colonies from soft agar after 12 weeks of carcinogen exposure were chosen.

These cells were isolated from soft agar, grown further in monolayer, until reaching large enough populations for further work, such as migration assay and RNA-isolation for molecular analyses. These transformed cell lines were also seeded in soft agar a second time to assure that the trait of anchorage independent growth was persistent. All these transformed cell lines also formed colonies in soft agar a second time.

Isolating cells from soft agar colonies was a difficult process with many critical steps. One single colony at the time was taken out from the soft agar and seeded in a single well in multi-well dishes to obtain clonal transformed cell lines (all cells originated from the same colony). It was the initial intention to isolate four colonies from each treatment that resulted in transformation after 12 weeks, but only cells from a subset of colonies survived and attached to the dish. Therefore, only 1-2 colonies were successfully isolated from each treatment. These transformed cell lines were each given its own name that will be referred to in the further analyses (Table 3.1). This table specifies the treatment that induced transformation and also which cell line (HBEC-2KT or HBEC-12KT) they are derived from. HBEC-2KT derived transformed cell lines are given the prename T2-, and HBEC-12KT derived transformed cell lines are given the prename T12-. The rest of the name specifies the exposure conditions: T2-CSC-L is transformed (T), derived from HBEC-2KT (2) after colony formation in soft agar and 12 weeks exposure to CSC, low concentration (CSC-L). In those cases where two transformed cell lines have been isolated from separate colonies, but the same cell line and treatment, they are given distinct numbers at the end of the name (T12-MNU-1 and T12-MNU-2).

Figure3.1: Transformed cell lines and their weekly treatment for 12 weeks. Which cell line (HBEC-2KT or HBEC-12KT) they are derived from are specified in the right column. Colonies obtained from the same treatment are given distinct numbers (1 and 2)

Transformed HBEC cell line	Treatment
T2-CSC-L	HBEC-2KT exposed to low dose CSC (1 µg/ml).
T2-CSC-H	HBEC-2KT exposed to high dose CSC (3 µg/ml).
T12-CSC-L1	HBEC-12KT exposed to low dose CSC (1 µg/ml) isolated from colony 1.
T12-CSC-L2	HBEC-12KT exposed to low dose CSC (1 µg/ml). isolated from colony 2.
T12-CSC-H	HBEC-12KT exposed to high dose CSC (3 µg/ml)
T12-B[a]P-L	HBEC-12KT exposed to low dose B[*a*]P (0,33 µM)
T12- B[a]P-H	HBEC-12KT exposed to high dose (1 µM B[*a*]P)
T12-MNU-1	HBEC-12KT exposed to MNU (1 mM) isolated from colony 1.
T12-MNU-2	HBEC-12KT exposed to MNU (1 mM) isolated from colony 1.

3.4 Proliferation assay.

Proliferation rate was measured during the exposure period on cells exposed to B[*a*]P and DMSO. In addition, proliferation rate was measured on the transformed cell line T2-CSC-L. The intention for measuring proliferation rate was to calculate how many replications the cells had been through during the exposure period, and to investigate if there were any changes in proliferation rate. Divisions/day was calculated and analyzed by one-way ANOVA test and Tukey post test. No significant changes in proliferation rates were observed during the weekly carcinogen exposures (Fig 3.6). T2-CSC-L did not show

any significant change in proliferation rate, when compared to the other HBEC-2KT cells, even though it was transformed. A significant difference between the two HBEC cell lines was observed, on the contrary, as suspected during the optimization experiments. HBEC-2KT has approximately twice as many divisions/day. This means that if HBEC-12KT cells have been through approximately 58.8 divisions in the 12 weeks exposure period (0.7 divisions /day · 84 days), HBEC-2KT have been through 117 division in the same time lapse (1.4 divisions /day · 84 days). This fact should be taken into consideration when analyzing results of further experiments, such as for example migration and gene expression.

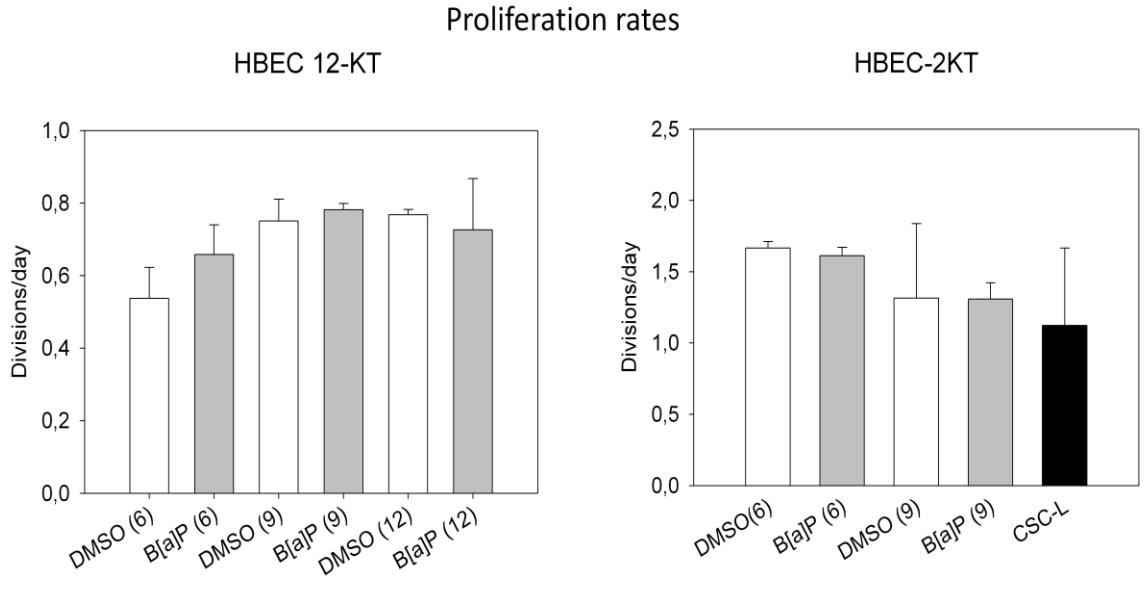

Figure 3.6: Divisions/day on HBEC-2KT and -12KT cells exposed to B[*a*]P or DMSO and the transformed cell line T2-CSC-L (black) Columns show the mean value SD. No differences in proliferation rate between controls (DMSO) and exposed cells were statistically significant (One-way ANOVA test with Tukey post-test).

3.4 Morphological changes during transformation.

HBECs originally have a rounded, epithelial shape when grown in monolayer and observed in the light microscope. Cellular morphology was inspected several times weekly during the carcinogen exposure regimen. The shape of some of the exposed cells changed dramatically during this period. The earliest changes were observed in HBEC-2KT exposed to CSC. These changes appeared after approximately three weeks exposure and in both doses of CSC. The cells acquired a more elongated shape, resembling a mesenchymal cell type. These were early indications that had activated the regulatory developmental program termed Epithelial-to-mesenchymal transition (EMT).

Similar changes were also observed in HBEC-12KT cell lines exposed to CSC, B[*a*]P and MNU, a few weeks later. Figure 3.7 illustrates the morphological differences between transformed cell lines and cells exposed to DMSO. The rounded, epithelial shape, which characterized both HBEC-2KT and HBEC-12KT exposed to DMSO is shown in (A) and (E), respectively. These photos are taken with low cell-density (A) and high cell-density (E), to illustrate that they maintained their rounded, epithelial shape, independent of cell-density. (B-F) shows transformed cell lines that have been isolated from three weeks in soft agar. Even though these morphological changes were observed as early as after three weeks of exposure, they maintained this elongated, mesenchymal shape several weeks after the removal of carcinogens.

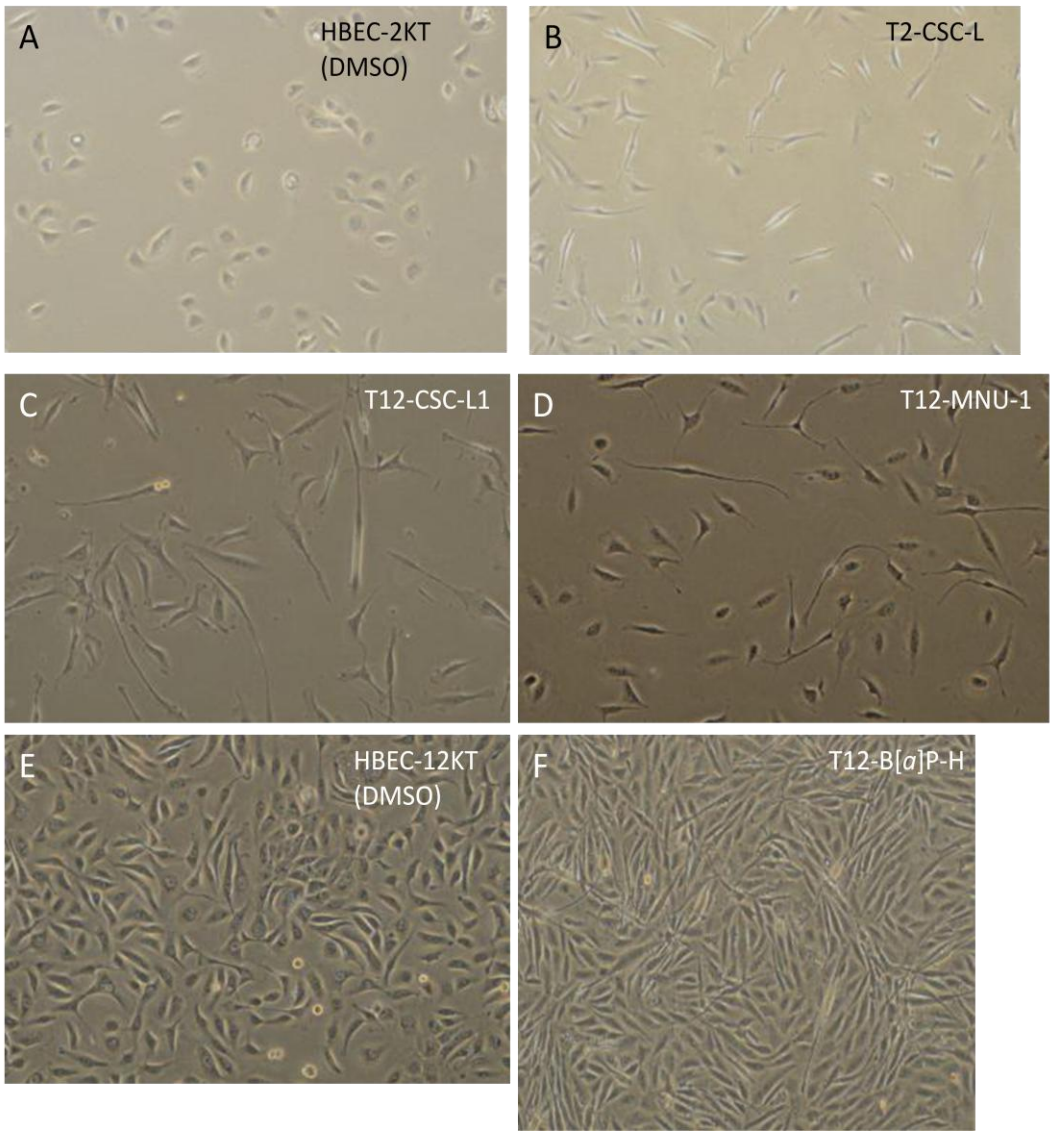

Figure 3.7: A) Original epithelial, rounded shape of HBEC-2KT cells. B) Elongated fibroblast-like shape of the transformed cell line T2-CSC-L, B and C) shows similar changes in the transformed T12-CSC-L1 and T12-MNU-1 cell line, E) HBEC-12KT with normal original shape exposed to DMSO for 12 weeks, and F) shows the transformed cell line T12-B[a]P-L .

In the following, a separate presentation of morphology will be given for HBEC-2KT derived transformed cell lines (T2-) and HBEC12-KT derived (T12-). For details about the transformed cell lines presented here, and their previous treatment, see Table 3.1. Starting with HBEC-2KT, as already described, early changes were observed in cells exposed to both doses of CSC. These changes were persistent during the exposure period and after removal of CSC. Figure 3.8 shows the original, rounded, epithelial shape of DMSO exposed cells (A), and transformed cells with an elongated, mesenchymal shape exposed to CSC (C-D). This figure also shows HBEC-2KT exposed to MNU for 12

weeks (B). These cells have maintained their epithelial shape similar to the DMSO-exposed cells. Also, the HBEC-2KT cells exposed to both doses of B[*a*]P maintained the epithelial shape. In conclusion, HBEC-2KT cells that acquired anchorage-independent growth and formed colonies in soft agar (transformed) also went through dramatic morphological changes, consistent with EMT. Those HBEC-2KT cells that were not transformed, on the other hand (DMSO, B[*a*]P and MNU), maintained their epithelial morphology.

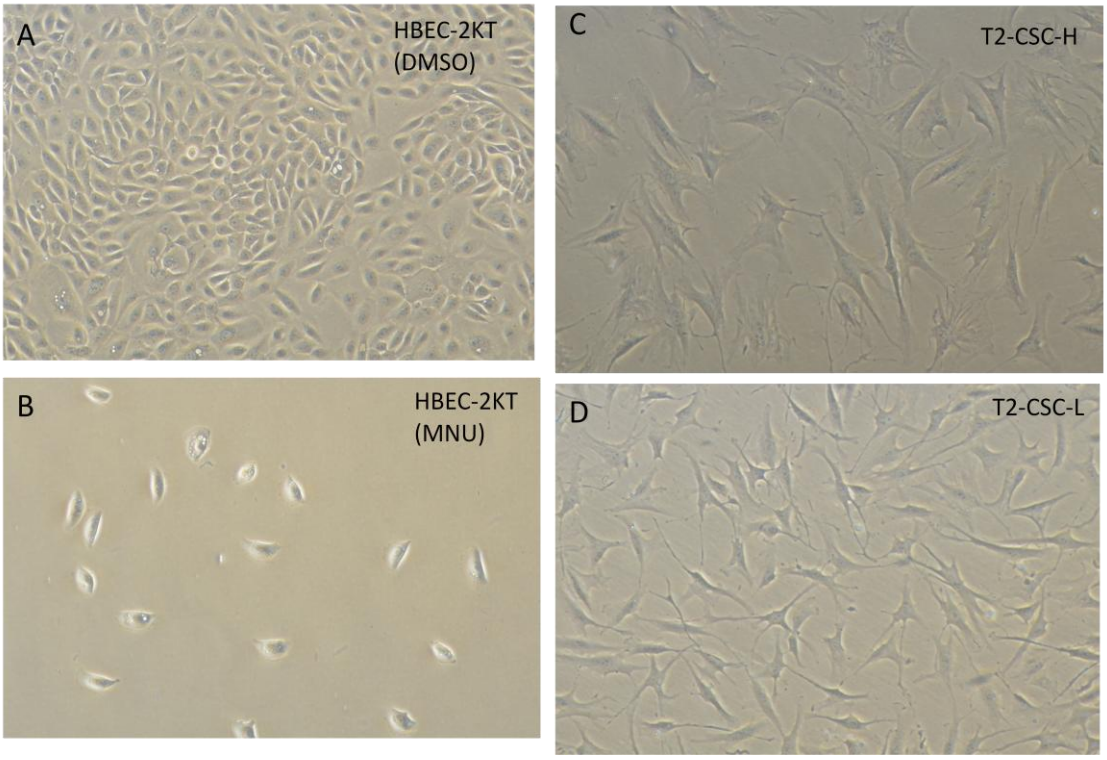

Picture 3.8: A and B) HBEC-2KT after exposure to DMSO and MNU, respectively. D and E) The transformed cell lines T2-CSC-H and T2-CSC-L.

Similar morphological changes were observed in most of the HBEC-12KT derived transformed cell lines (T12). As shown in Figure 3.7, T12-CSC-L and T12-MNU-1 went through a dramatic change in morphology. The same changes were observed for T12-CSC-L2 and T12-MNU-2, but surprisingly, T12-CSC-H maintained an epithelial morphology. So did T12-B[*a*]P-L (Fig 3.9). In conclusion, not all transformed HBEC-12KT changed their morphology, but even though some of the transformed T12- cell lines did not have a typically mesenchymal appearance, they may represent intermediate stages in EMT.

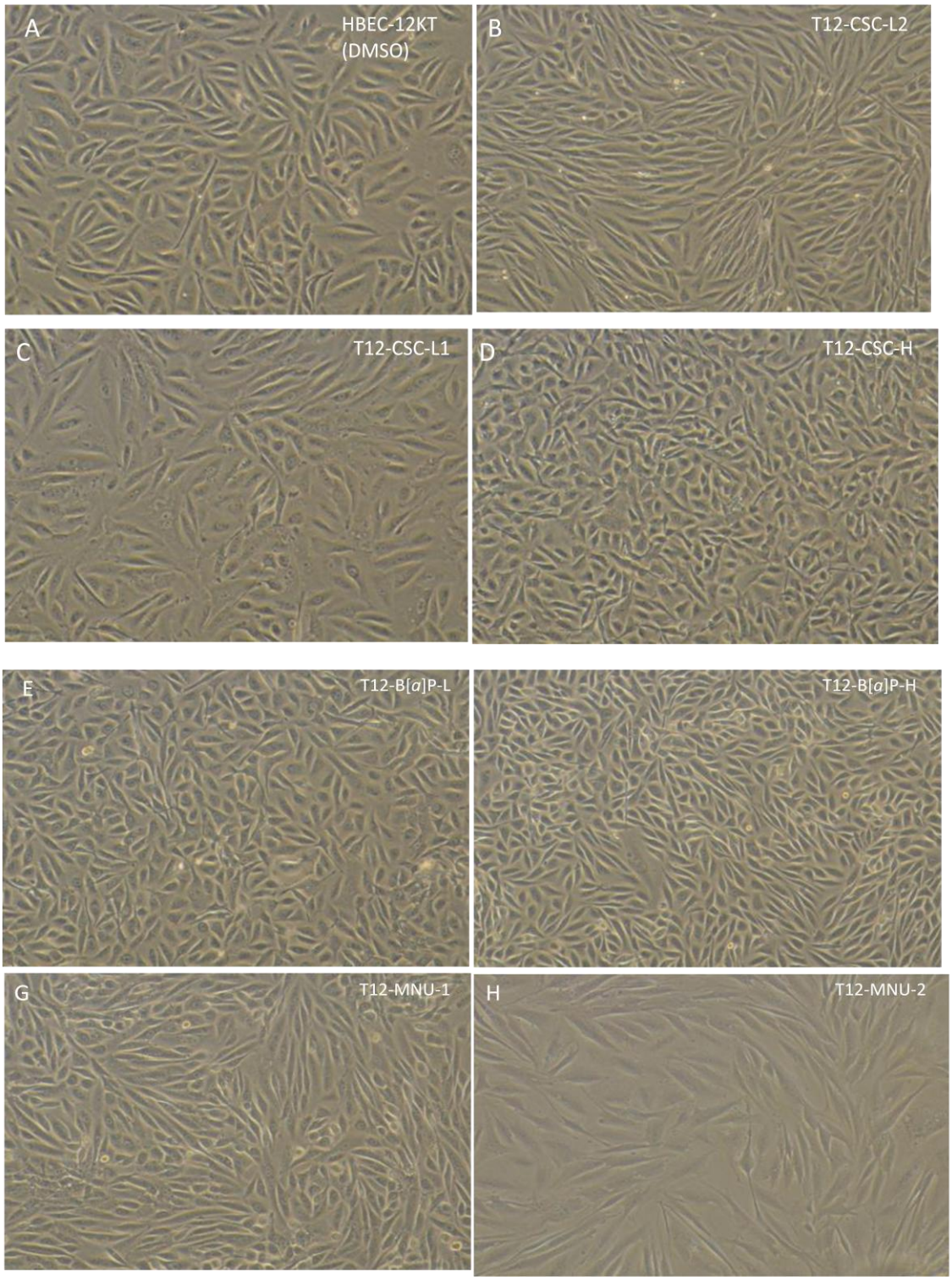

Figure 3.9: A) HBEC-12KT exposed to DMSO with the original, epithelial shape. B- H) Transformed HBEC-12KT (T12-).

In addition to morphological changes, consistent with EMT, overlapping growth was observed in several of the transformed cell lines of both HBEC-12KT and HBEC-2KT,

indicating loss of contact inhibition (see Figure 3.10). This trait was never observed in control cells (DMSO).

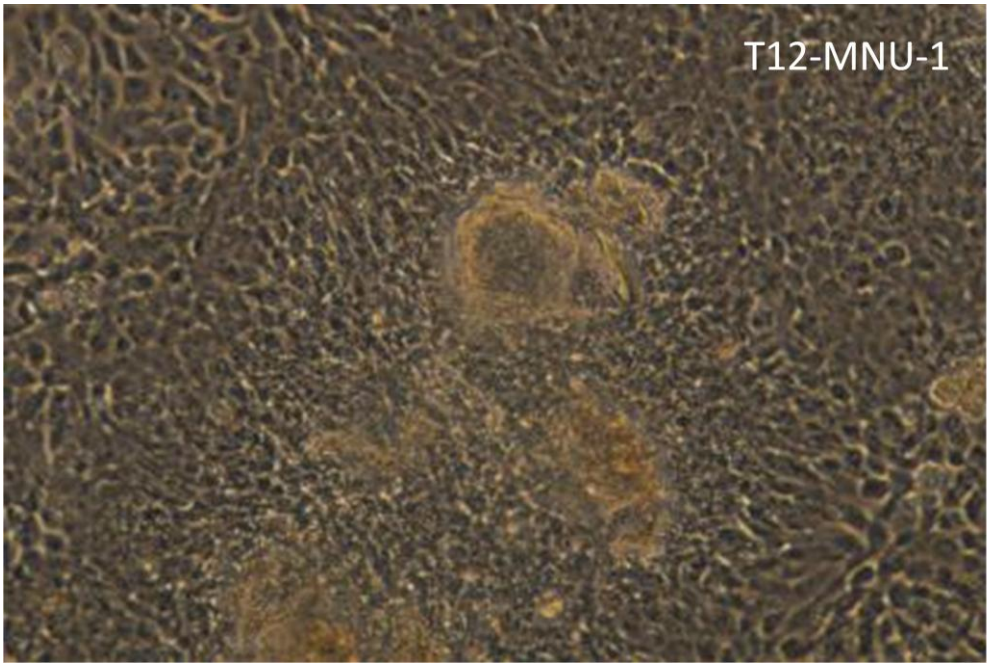

Figure 3.10: Transformed cells (T12-MNU-1) with overlapping growth.

3.5 Migration assay

Increased cellular motility and migration capability is a characteristic associated with EMT. This migration assay is also called wound-healing assay because it is used to investigate cells ability to migrate into an experimentally applied open wound in the cell layer, and thereby wound-healing. Several of the transformed cell lines had a dramatic change in morphology in agreement with EMT, and the migration assay was performed to investigate those characteristics further.

Migration capability was tested on a subset of the transformed cell lines in comparison to HBECs exposed to DMSO for 12 weeks. Figure 3.11 shows the results from the transformed cell line T2-CSC-L. The figure shows pictures taken just after scratching (1A and B), and 24 hour later (2a and b). After 24 hour, the transformed cell line T2-CSC-L had completely filled the gap, while DMSO exposed cells had only slightly moved. The figure also illustrates, from a different experiment, how the migrating cells fill the open wound (3). In conclusion, the tested transformed cell line (T2-CSC-L) had gained an increased ability to migrate when compared to DMSO exposed cells.

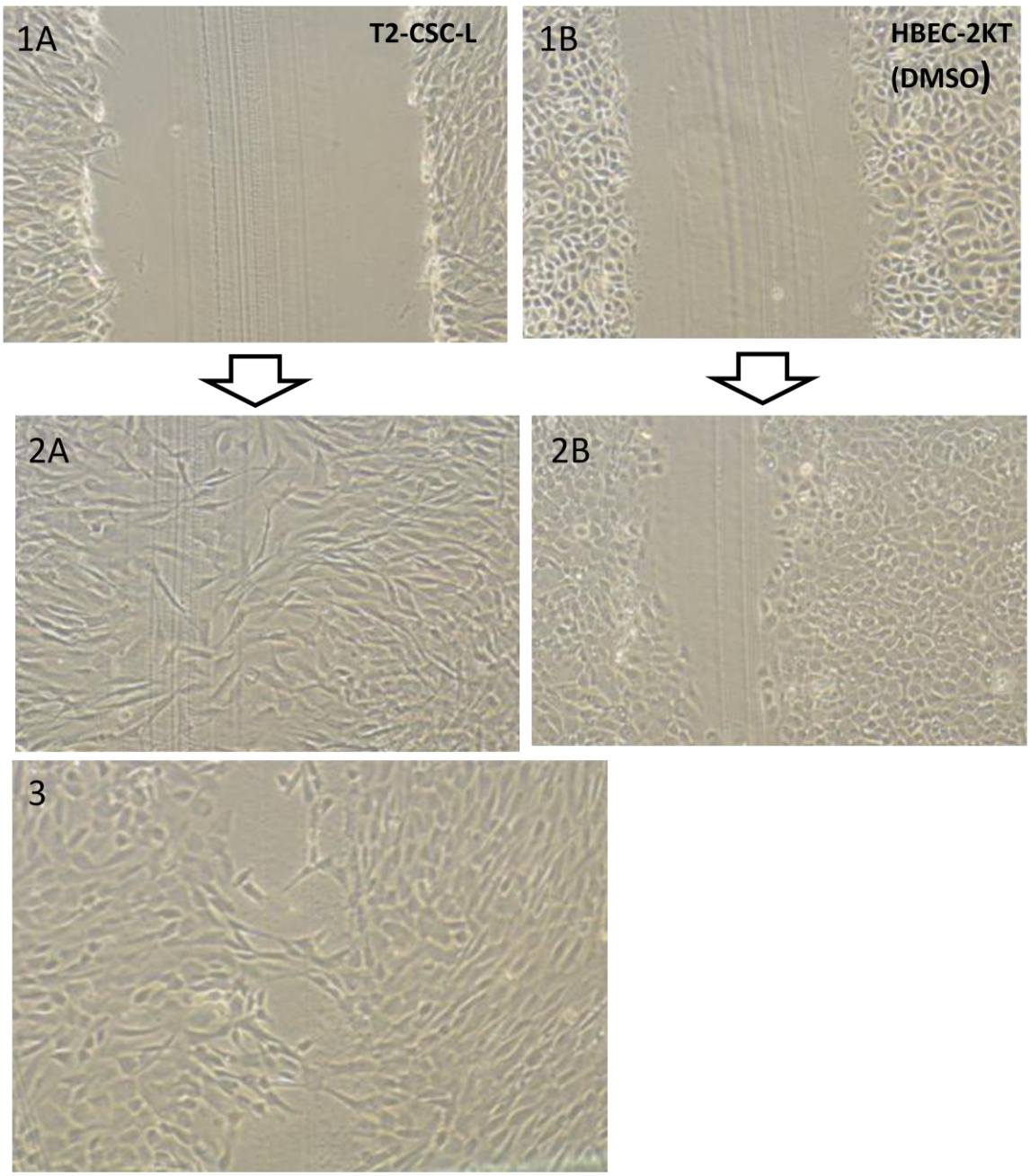

Figure 3.11: 1A and B) T2-CSC-L and DMSO exposed cells, just after scratching, 2A and 2B) Cells 24 hours later, and 3) migrating T2-CSC-L cells from a different experiment.

3.6 Gene expression analysis

RT-qPCR was performed on transformed cell lines (see Table 3.1) in comparison to control cells exposed to DMSO (12 weeks). RT-qPCR was performed on genes involved in EMT, carcinogen-metabolism and steroid receptor pathways. No changes were observed in the expression of *CYP1A1, CYP1B1* and *AHR*. These results are shown in the Appendix E.

Figure 3.12 shows gene expression of the two genes encoding the cadherins *CDH1* (E-cadherin) and *CDH2* (N-cadherin). The cadherin-switch, from E-cadherin (*CDH1*) to N-

cadherin (CDH2) is a molecular hallmark of EMT. In both T2-cell lines, *CDH1* expression was strongly reduced, whereas *CDH2* expression was strongly induced, in accordance with an EMT. *CDH1* expression was significantly reduced in five of the seven transformed T12- cell lines, while two of these cell lines did not show reduced expression. Four of the T12-cell lines had significantly increased expression of *CDH2* and there was a tendency towards increased expression in the two other cell lines, but these were not significant. Overall, there were indications of a cadherin-switch in the T12-cell lines, as well. However, in a few of them, there were no clear indications of an abnormal expression of the cadherin genes, even though these cell lines were transformed.

In addition to the cadherin switch, changes in cellular morphology and increased migration capability characterize the EMT program. Both of the T2-cell lines had a dramatic change in morphology and a highly increased migration capability. In these two cell lines there was a strong correlation between the cadherin switch, morphology and migration capability. In T12-cell lines, some cell lines did not follow the EMT pattern. Both of the T12-B[*a*]P cell lines and T12-CSC-H maintained their epithelial morphology. In T12-B[*a*]P-H, *CDH1* was not downregulated which at least partly may explain the epithelial phenotype. In T12-CSC-H and T12-B[*a*]P-L *CDH1* was downregulated, but these cell lines still have maintained an epithelial morphology.

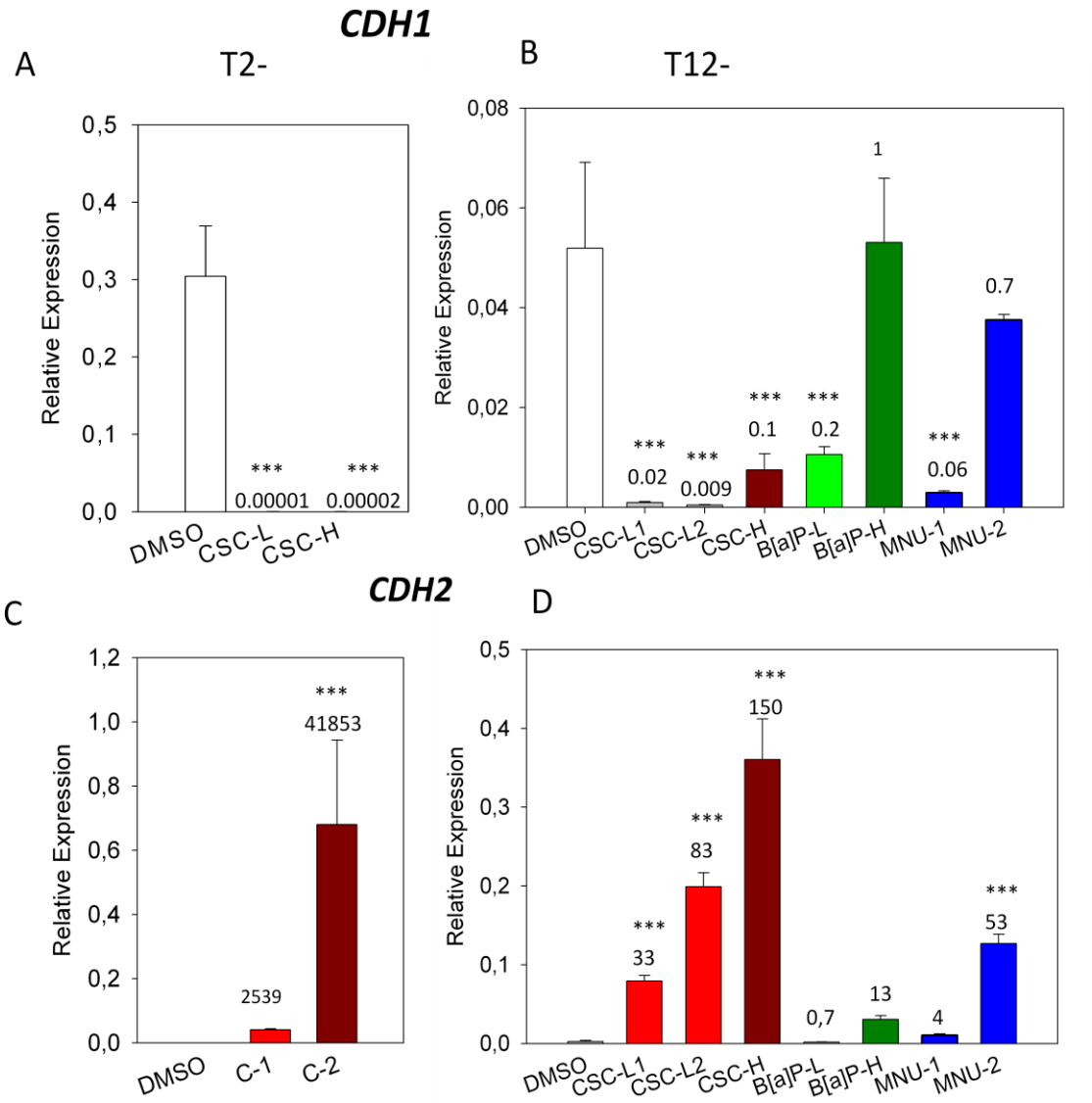

Figure 3.12: ***CDH1*** **and** ***CDH2*** **gene expression in transformed cell lines. Columns show the mean value SD. Fold changes compared to DMSO are shown over each column. One-way ANOVA test with Tukey post test was performed and the following p-values are marked: p<0,05=*, p<0,01=**, p<0,001=***. A) and B) shows expression of** ***CDH1*** **and C) and D) expression of** ***CDH2*** **in HBEC-2KT and HBEC-12KT derived cell lines, respectively. In all cases gene expression levels were normalized to the expression of** ***β-actin*****.**

Figure 3.13 shows gene expression of *AR, ERα* and *ERβ* on the transformed cell lines. The expression of *AR* was significantly upregulated in six of nine transformed cell lines. The remaining three also showed a tendency of increased expression, but this was not significant. *ERα* is not expressed in DMSO exposed HBEC-2KT or T2-cell lines. In two T12 cell lines *ERα* is significantly upregulated, and in two others there is a tendency, but not significant, upregulation of *ERα. ERβ* was significantly upregulated in four of nine transformed cell lines. Three of the remaining cell lines also showed a tendency of increased expression, but this was not significant. T2-CSC-L showed a small, but significant reduction of *ERβ* expression. Overall, there are indications of increased expression of *AR, ERβ* and partly also *ERα* during *in vitro* transformation. This indicates that the steroid receptors may be involved in the transformation process.

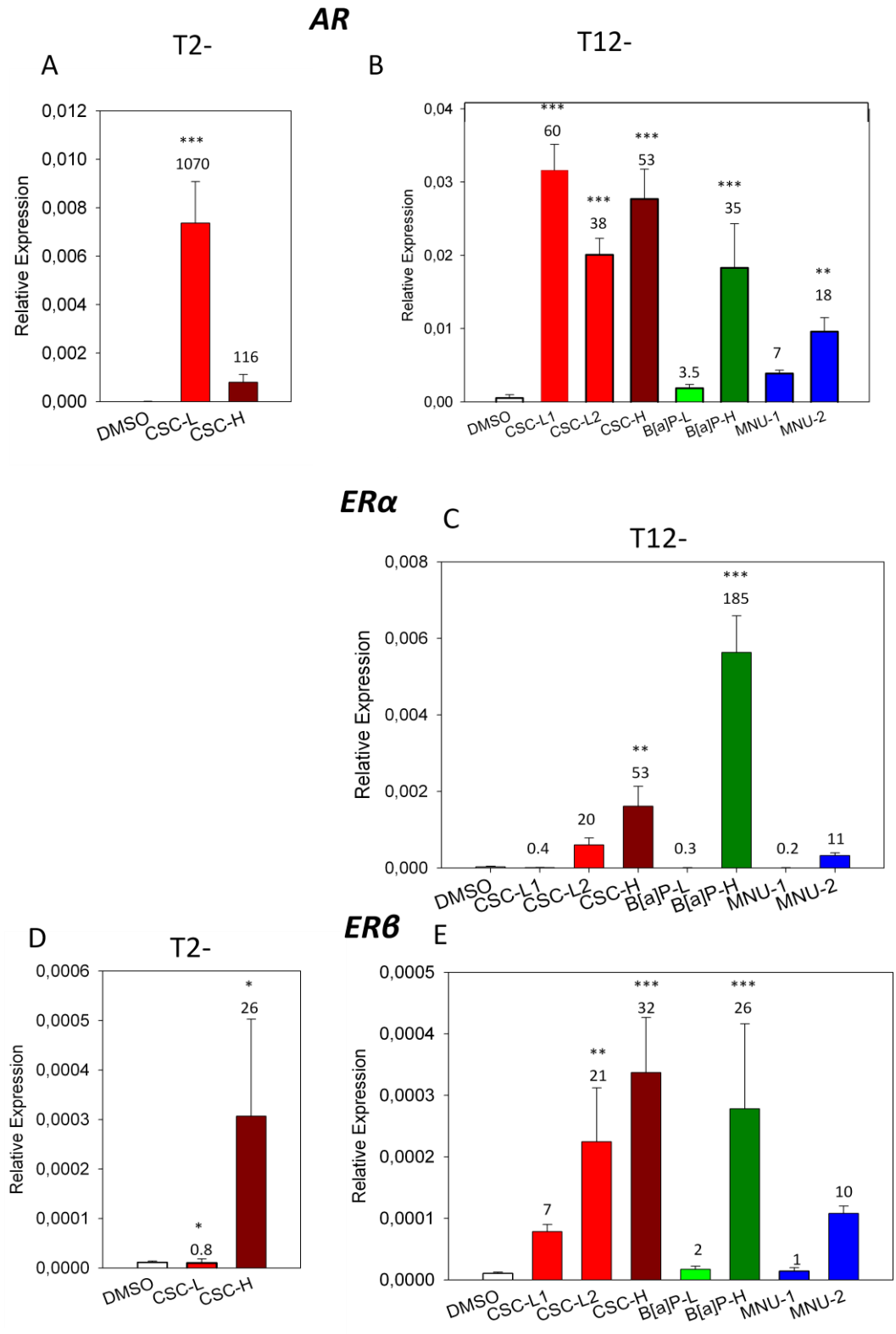

Figure 3.13: *AR, ERα* and *ERβ* gene expression in transformed cell lines. Columns show the mean value SD. Fold changes compare to DMSO are shown over each column. One-way ANOVA test with Tukey post test is performed and the following p-values are marked: p<0,05=*, p<0,01=, p<0,001=***. A) and B) shows expression of *AR*, C) Expression of *ERα* and D) and E) expression of *ERβ* in HBEC-12KT derived cell lines, respectively. In all cases gene expression levels were normalized to the expression of *β-actin*.**

Figure 3.14 shows gene expression of *FOXA1, FOXA2* and *GREB1*. *FOXA1* was significantly downregulated in T2-cell lines, but upregulated in most of the T12-cell lines. Four of these changes are significant, while two T12-cell lines show a small and unsignificant reduction. *FOXA2* is significantly downregulated in T2-cell lines. This gene is moderately induced in one cell line (T12-B[*a*]P), reduced in three (T12-CSC-L) (T12-MNU-1 (T12-MNU-2), but unaltered in the remaining three.

GREB1 was expressed in HBEC-2KT exposed to DMSO, but not in T2-cell lines. Therefore no statistics is performed on these results, but a downregulation can be assumed. Three of the T12-cell lines showed increased expression of *GREB1.* Overall, *FOXA1* showed opposite changes in T2- and T12- cell lines. *FOXA2* was mostly downregulated with the exception of (T12-B[*a*]P), whereas *GREB1* also showed opposite changes in T2- and T12-cell lines. The expression of *GREB1* appears to largely follow the pattern of *FOXA1* closely, in both T2- and T12-cell lines.

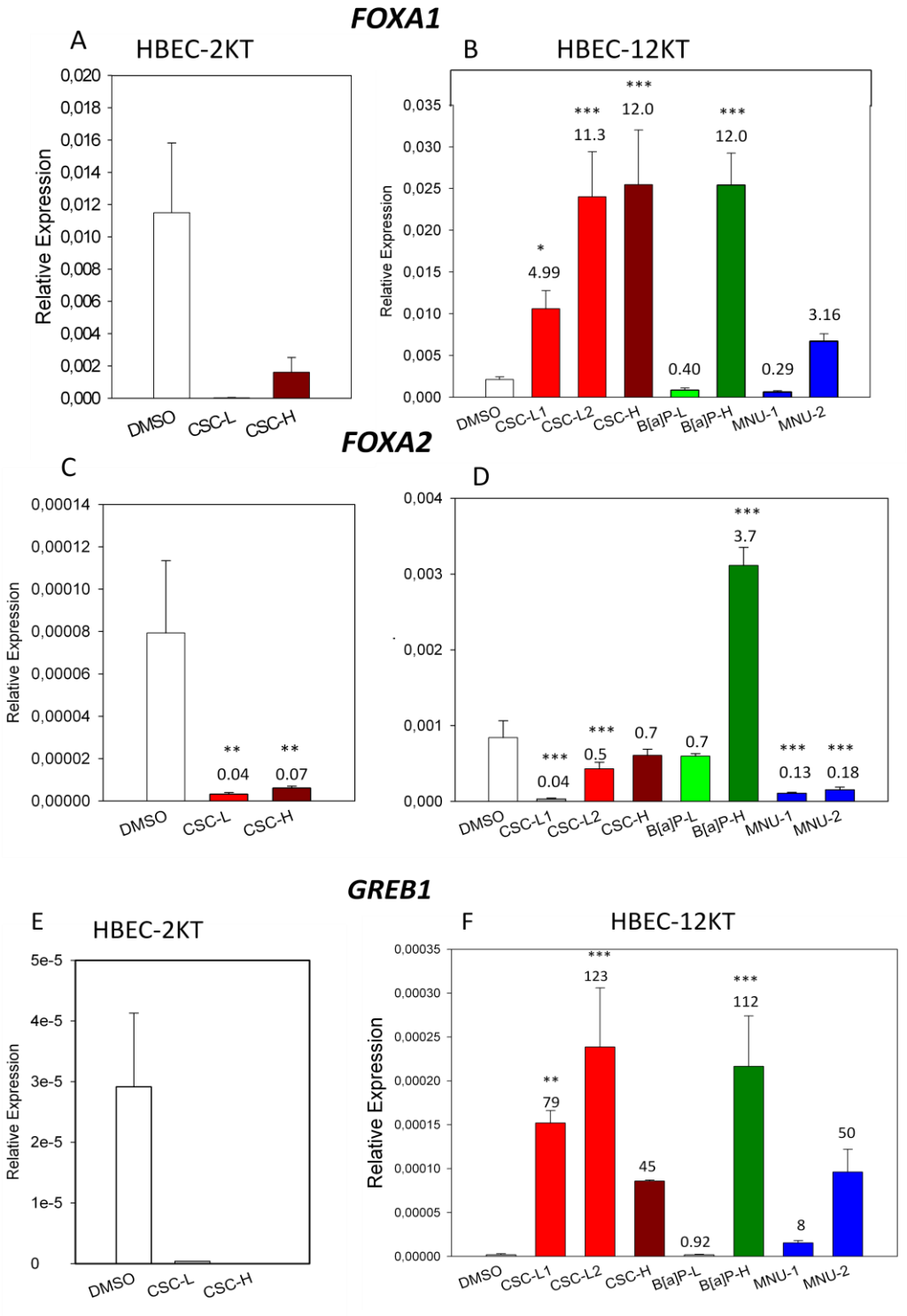

Figure 3.14: *FOXA1* and *FOXA2* gene expression in transformed cell lines. Columns show the mean value SD. Fold changes compared to DMSO are shown over each column. One-way ANOVA test with Tukey post test was performed and the following p-values are marked: p<0,05=*, p<0,01=, p<0,001=***. A) and B) shows expression of *FOXA1*, C) and D) Expression of *FOXA2* and E) and F) Expression of *GREB1* in HBEC-2KT and HBEC-12KT derived cell lines, respectively. In all cases gene expression levels were normalized to the expression of β-actin.**

3.7 DNA methylation assay

Exposure to the DNA demethylating agent decitabine was performed on T2-CSC-L which showed reduced expression of *FOXA1* and *FOXA2*. The result from RT-qPCR on *FOXA1* is shown in Appendix F. *FOXA2* was not expressed after exposure. No effect on the decitabine treatment on *FOXA1* or expression was observed. RT-qPCR results on *FOXA2* showed no expression this gene. More experiments need to be performed before it is possible to conclude from these results since it was only performed once and on one of the transformed cell lines.

3.8 miRNA expression

The expression of miR-27a, miR-21, and miR-24 was measured by RT-qPCR. miRNA RT-qPCR results were first analysed by normalizing to *β*-actin (Fig. 3.15, left column). Further analyses showed that the observed changes in gene expression were probably mostly due to changes in *β-actin*. Therefore these results are also presented as Cq-values, only (Fig 3.15, right column). There were only small changes in the expression of these three miRNA both with or without normalization to β-actin. Statistics were eonly performed on the Cq-vulues, most of the the changes were not significant. Thus, based on these results, changes in miR-27a, miR-21 and miR-24 do not appear to be involved in *in vitro* transformation of HBEC cells. However, as in the case of DNA methylation assay, these experiments need to be repeated before we are able to conlude.

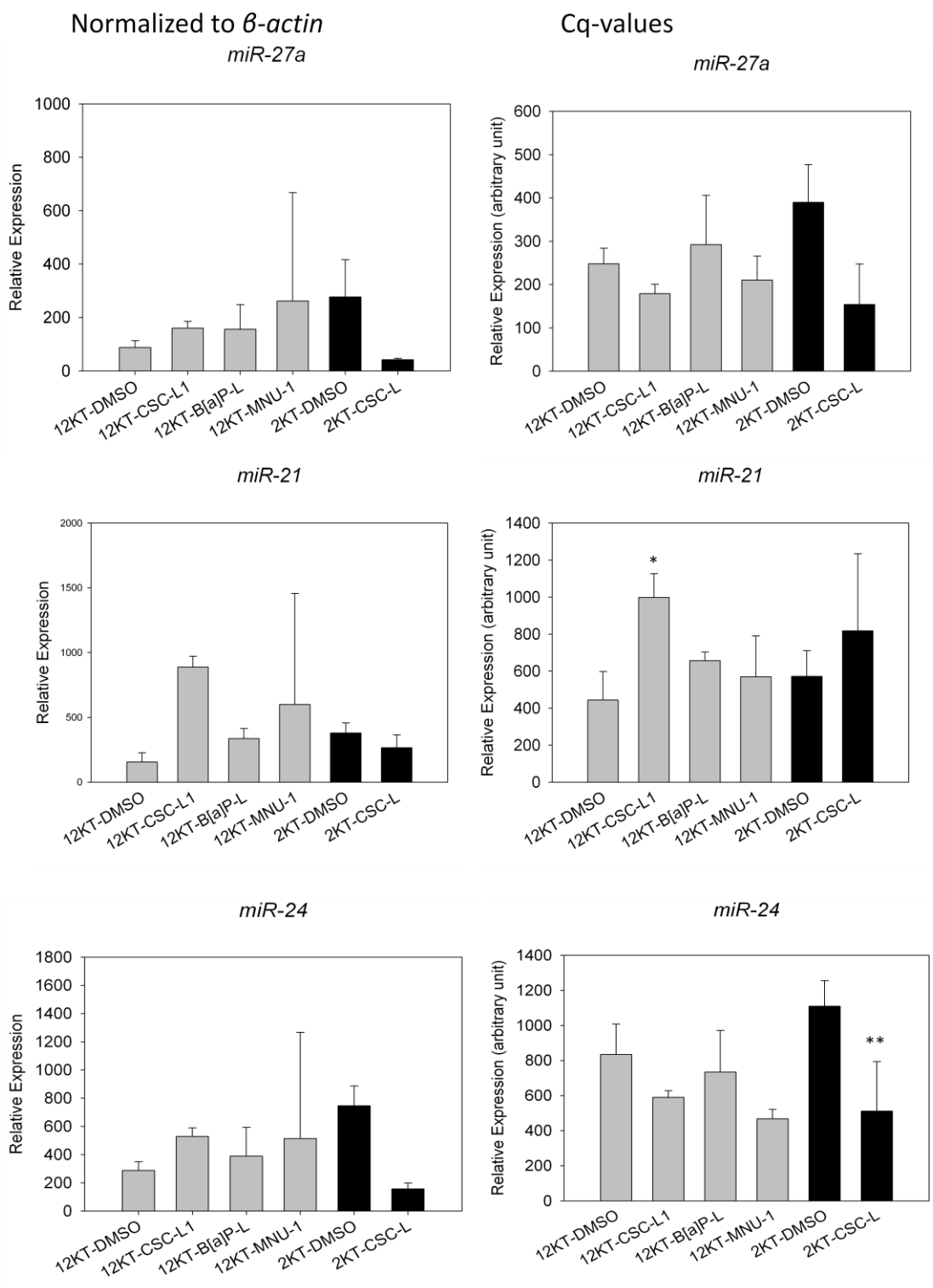

Figure 3.14: Results from miRNA RT-qPCR. Columns show the mean value SD. One-way ANOVA test with Tukey post test is performed and the following p-values are marked: p<0,05=*, p<0,01=. Statistics is only performed on the Cq-values.**

4 Discussion

The aim of this study was to investigate early molecular changes during premalignant cell transformation. Steroid receptor pathways have been hypothesized to be involved in lung carcinogenesis, possibly by interacting with carcinogen metabolism, and by interfering with cellular signaling pathways related to control of cell proliferation (Berge, Mollerup et al. 2004). Epithelial-to-mesenchymal transition (EMT) has also recently been found to be induced by carcinogens at early stages of lung carcinogenesis (Tellez, Juri et al. 2011).

In vitro studies of early changes during lung carcinogenesis have been restricted by the cell lines available, but HBECs were recently immortalized by insertion of Cdk4/hTERT (Ramirez, Sheridan et al. 2004). These cells have few genetic alterations and are therefore a new valuable tool for studying early changes *in vitro*. In this study, these cell lines were used in an *in vitro* transformation model to investigate if molecular changes involved in steroid receptor pathways, carcinogen metabolism, and EMT was associated with premalignant transformation.

In addition to epidemiological, clinical, and animal studies, *in vitro* studies are important tools for investigating carcinogenesis. There are, of course, weaknesses associated with *in vitro* model systems. The carcinogenic process is extremely complex. An *in vitro* transformation model simplifies parts of this process and one should be careful jumping from conclusions found in this system to conclusions about human lung carcinogenesis. But, together with knowledge from other approaches, it provides a model that can give valuable new insight into lung carcinogenesis.

Cell lines used for long-term *in vitro* studies need to have a long-term replicative potential. Since primary human bronchial epithelial cell lines have a finite replicative potential, they need to be immortalized in order to become long-term replicating cultures. Immortalization is often accomplished by introduction of oncogenes or silencing of tumor suppressor genes. Many immortalized cell lines therefore do not have an intact p53 checkpoint and often become genomically unstable after several passages. Genomic instability characterizes later steps of carcinogenesis - cancer progression. *In vitro* models to study early premalignant changes therefore have been restricted by the

lack of cell lines with few genetic changes. Since Cdk4/hTERT-immortalized HBECs have an intact p53 checkpoint, are genomically stable, and have few genetic alterations, they may be more suitable than many other immortalized cell lines as models to study premalignant changes (Gazdar, Gao et al. 2010).

In this *in vitro* transformation model, the doses of tobacco carcinogens were intended to be low, compared to the doses used in many other *in vitro* transformation models (Veljkovic, Jiricny et al. 2011). This was to mimic the situation occurring in the bronchial epithelium of the smoker as close as possible. But still, the carcinogen doses are much higher than those occurring in the bronchial epithelium of the smoker. This is because cancer development is a long-term process, most often requiring decades of smoking exposure to develop. After long-term *in vitro* exposure, the cells were seeded in soft agar to test for colony formation. Anchorage independent growth, evident by colony formation in soft agar, has been considered one of the hallmarks of transformation and was therefore used in this model to select for transformed cells. HBEC cell lines do not form colonies in soft agar at the starting point. Therefore, cells that formed colonies were defined as transformed.

The first goal in this study was to establish an *in vitro* transformation model and to test if HBECs could be transformed by exposure to CSC, B[*a*]P or MNU. Earlier studies have reported CSC-induced transformation with the human bronchial epithelial cell line BEAS2B (Veljkovic, Jiricny et al. 2011). Since this cell line is immortalized by using viral oncoproteins (Reddel, Ke et al. 1988), and often become spontaneously malignant after several passages without any exposures, transformed BEAS2B may be more suitable as models to study molecular changes involved in later stages of lung carcinogenesis. HBECs have previously been transformed by exposure to MNU and the ultimate carcinogen of B[*a*]P - BPDE (Damiani, Yingling et al. 2008). Since B[*a*]P needs to be bioactivated by carcinogen metabolizing enzymes into BPDE in order to induce DNA damage, our model also tested the capacity of HBECs to bioactivate B[*a*]P sufficiently for transformation. The results obtained in this study show for the first time that HBECs have the ability to bioactivate B[*a*]P sufficiently for transformation. This requires the presence of CYP enzymes and probably also high induction of these enzymes through the AHR (Uppstad, Ovrebo et al. 2010). It should be noted that only one of the tested

HBEC cell lines (HBEC-12KT) were transformed by exposure to B[*a*]P. This may be due to experimental conditions, or it may be due to the fact that there is large inter-individual variability in the level of CYP1A1 induction (Jacquet, Lambert et al. 1996).

The next goal was to isolate cells from soft agar colonies that could be established as transformed cell lines. These transformed cell lines were then further used as models to investigate molecular changes during transformation. Gene expression analyses were performed on these transformed cell lines, in comparison to HBEC cell lines exposed to DMSO for the same period of time and under the same conditions. Nine different transformed cell lines derived from HBEC-2KT and HBEC-12KT were established after different treatments and many of them had changed their morphology.

The morphological shape of the cells in most of the carcinogen treatments changed into an elongated, mesenchymal-like shape, while others maintained the original, rounded, epithelial shape. These morphological changes turned out to be largely associated with transformation. Most of the cells that changed into a mesenchymal-like cell type, also acquired the capability of anchorage independent growth, evident by colony formation in soft agar. These morphological changes suggested that the transformed cells had activated the regulatory developmental program EMT (Kalluri and Weinberg 2009). To investigate this hypothesis further, their migration capability was tested. Increased motility and migration are hallmark phenotypes of EMT. Those transformed cell lines that were tested, showed an increased motility and migration. Downregulation of *CDH1* (encoding E-cadherin) and upregulation of *CDH2* (encoding N-cadherin), the so-called cadherin switch, has been considered the molecular hallmark of EMT. RT-qPCR measurement of gene expression revealed that most of the transformed cells, showed a reduced expression of *CDH1* and an increased expression of *CDH2*. These results confirmed that EMT was activated in this premalignant *in vitro* transformation. EMT has earlier been associated with later steps of carcinogenesis, but recent studies suggest that this program also can be activated during premalignant stages (Tellez, Juri et al. 2011). The results obtained in this study support these findings.

Overlapping growth was also observed in several of the transformed cell lines after recovering from soft agar. Overlapping growth is associated with loss of contact

inhibition. This has been considered an *in vitro* surrogate of a mechanism that operates *in vivo* to maintain tissue homeostasis. A protein known as Merlin orchestrates contact-inhibition via coupling cell surface molecules, such as E-cadherin to their transmembrane receptor tyrosine kinases. Merlin thereby strengthens the adhesivity of cadherin-mediated cell-to-cell attachments (Hanahan and Weinberg 2011) In conclusion, overlapping growth is also a trait associated with transformation.

Gene expression analyses performed on the nine transformed cell lines showed no significant changes in the expression of *CYP1A1, CYP1B1* and *AHR.* It has previously been shown that *CYP1A1* and *CYP1B1* is of major importance in the bioactivation of B[*a*]P in human lung cell lines, and that exposure to B[*a*]P induces expression of *CYP1A1* and *CYP1B1* (Uppstad, Ovrebo et al. 2010). In this transformation assay, only permanent molecular changes were tested. After the exposure period was finished, and the carcinogens removed, several weeks passed before the cells were harvested for RNA-isolation and gene expression measurements. Considering the rapid turnover of *CYP1A1* mRNA (McLemore, Adelberg et al. 1990), this may explain why no significant changes were observed in these genes.

Steroids are involved in carcinogenesis through several mechanisms. Estrogen can stimulate cell signaling and proliferation in the breast via ER pathways (Yager and Davidson 2006), and androgens enhance DNA damage and oxidative stress during hepatocarcinogenesis (Ma, Hsu et al. 2008). Epidemiological and molecular studies indicate that females may be more susceptible than males to tobacco smoke carcinogens (Zang and Wynder 1996; Haugen 2002; Siegfried, Hershberger et al. 2009). It has therefore been suggested that steroid receptor pathways are involved in lung carcinogenesis, possibly through an interaction with carcinogen metabolism. There is large inter-individual variability in the level of *CYP1A1* induction, and high *CYP1A1* induction has been considered a risk factor for lung cancer (Jacquet, Lambert et al. 1996). Previous studies have shown a higher level of *CYP1A1* gene expression and PAH-related DNA adducts among female lung cancer patients (Mollerup, Ryberg et al. 1999). *In vitro* studies suggest complex interactions between ER and AHR pathways (Thomsen, Wang et al. 1994). Such interactions may be involved in explaining the higher level of *CYP1A1* mRNA among female lung cancer patients. In this study, we wanted to test if

changes in the expression of steroid receptors were associated with the carcinogen induced transformation. Our results show that AR, ERβ, and partly also ERα were upregulated in the transformed cell lines. In conclusion, upregulation of steroid receptors may be associated with carcinogen induced transformation.

The transcription factors FOXA1 and FOXA2 are involved in regulating steroid receptor activity. Because we have an interest in steroid receptor pathways in relation to carcinogen metabolism gene expression of these transcription factors was also measured. FOXA factors may be a link between steroid receptors and carcinogen metabolism. In liver cancer, genes regulated by FOXA factors and steroid receptors clustered in the pathways controlling carcinogen metabolism (Li, Tuteja et al. 2012). Besides, these transcription factors have recently been found to be involved in several cancers. In human breast and prostate cancer cell lines, the recruitment of ERα or AR, receptively, depends on FOXA1 (Carroll, Liu et al. 2005). FOXA1 and FOXA2 are also thought to be important for sex differences in liver cancer, where estrogen has a protective effect, and androgen a deleterious effect (Kongsuwan, Knox et al.). Little is known about the FOXA transcription factors in lung cancer. We found that changes in the expression of *FOXA1* and *FOXA2* were associated with carcinogen induced transformation. FOXA1 was found to be upregulated in HBEC-12KT derived cell lines. This is in accordance with one earlier study performed on *FOXA1* and lung cancer in which it was found that FOXA1 was overexpressed and amplified in lung adenocarcinomas (Lin, Miller et al. 2002 . In HBEC-2KT derived cell lines, on the contrary, *FOXA1* was downregulated. *FOXA2* was mostly downregulated in the transformed cell lines. This is in support of a recent study, where it was found that FOXA2 was frequently downregulated in lung cancer.

The FOXA factors may also form a possible link between steroid receptors pathways and EMT. FOXA2 has been found to act as a suppressor of EMT in human lung cancers. Abundance of FOXA2 has been shown to be positively correlated with an epithelial phenotype, and negatively correlated with the mesenchymal phenotype (Tang, Shu et al. 2011). Consistently, knockdown of *FOXA2* promoted EMT in lung cancer cells, whereas overexpression of *FOXA2* reduced EMT. Also, in pancreatic cancer, loss of FOXA1/2 is essential for the EMT. In pancreatic ductal adenocarcinoma cell lines, forced inhibition of

FOXA1/2 has been shown to be sufficient to induce EMT (Song, Washington et al. 2010). E-cadherin has been called the “gatekeeper of the epithelial phenotype” and it is shown that FOXA1/2 overexpression can overcome several repressive signals of *CDH1* (E-cadherin gene) expression. Our results from gene expression analyses performed on transformed cell lines show that both *FOXA2* expression and *CDH1* expression was downregulated, in comparison to untransformed DMSO-exposed cells. The exception was T12-B[*a*]P-H which showed an increased expression of *FOXA2*. Interestingly, this transformed cell line is the only cell line that does not show any tendency of downregulation of *CDH1*. This support the hypothesis that increased *FOXA2* expression may overcome other suppressive mechanisms of E-cadherin. Overall, the gene expression analyses and morphological observations all show an association between a change in morphology, reduced *FOXA2* expression and reduced E-cadherin expression.

Another gene that may be involved in steroid receptor activity is *GREB1. GREB1* is an ERα target gene and is critically involved in the estrogen induced growth of breast cancer cells, (Chand, Wijayakumara et al. 2012). Little is known about *GREB1* in lung cancer. Our results show that *GREB1* was upregulated during carcinogen induced transformation of HBECs. Interestingly, the expression of *GREB1* in the different transformed cell lines seem to follow the expression of *FOXA1.* In HBEC-12KT derived cell lines also ERβ also follows this pattern. The fact that *GREB1* is significantly upregulated in several of the transformed cell lines indicates that this gene may also be involved in lung cancer, but its role needs to be investigated further.

Epigenetic mechanisms are highly involved in lung carcinogenesis and also in several of the processes described in this study. The mechanism of downregulation of *FOXA2* in lung cancer has been found to primarily be promoter hypermethylation (Basseres, D'Alò et al.). DNA-methylation assay followed by gene expression analyses performed in our study did not support that promoter hypermethylation was responsible for downregulation of *FOXA1,* but these experiments needs to be repeated. A recent study found that miR-200 familiy and miR205 was associated with EMT during carcinogen induced transformation of human lung epithelial cells (Tellez, Juri et al. 2011). MiR-21 is one of the most studied miRNAs in cancers, and is overexpressed in the most solid tumors, promoting progression and metastasis (Tian, Tu et al. 2012). MiR-21 expression

was tested on the transformed cell lines in this study. Only small changes were observed in the expression of miR-21, or the other miRNA that was tested (miR-24 and miR-27a) and mostly not significant.

In conclusion, an *in vitro* transformation model was successfully established in this study. It was shown that HBECs are capable of bioactivating indirect-acting carcinogens, such as B[*a*]P, sufficiently for transformation. Exposure to other tobacco smoke carcinogens also resulted in transformation. By using these transformed cell lines in further studies we found that changes in the expression of steroid receptor pathway members, including *FOXA1/2,* changed during carcinogen induced transformation. An upregulation of steroid receptors was observed. This indicates that steroid receptors pathways may be involved in lung carcinogenesis. In addition, an activation of EMT was observed during this premalignant transformation, and a downregulation of *FOXA2.* These results also lend support to the hypothesis that *FOXA2* may also be involved in regulating EMT.

For further work, the transformed cell lines from this study can be tested for their tumorigenic potential by subcutaneous injection in nude mice. Cells were also harvested after 6, 9 ,12 and 15 weeks of exposure for protein and DNA analyses, and cDNA is already made from cells exposed to carcinogens for 6, 9 ,12 and 15 weeks. It would be interesting to test gene expression of steroid receptors on HBEC-2KT cells exposed to B[*a*]P that did not become transformed. Are their steroid receptors also upregulated?

In addition, the establishment of an *in vitro* transformation model can be valuable also for testing other chemicals and investigate changes in morphology, EMT and gene expression after exposure and possibly transformation. Especially, a similar *in vitro* transformation of HBECs, but with the presence of steroid receptors and FOXA factor inhibitors would be interesting. If the presence of inhibitors of steroid receptor pathways could inhibit transformation, this would be very interesting for therapeutic purposes.

References

(2004). "Tobacco smoke and involuntary smoking." IARC Monogr Eval Carcinog Risks Hum **83**: 1-1438.

Augello, M. A., T. E. Hickey, et al. (2011). "FOXA1: Master of steroid receptor function in cancer." EMBO Journal **30**(19): 3885-3894.

Baek, D., J. Villén, et al. (2008). "The impact of microRNAs on protein output." Nature **455**(7209): 64-71.

Bartel, D. P. (2009). "MicroRNAs: target recognition and regulatory functions." Cell **136**(2): 215-233.

Basseres, D. S., F. D'Alò, et al. "Frequent downregulation of the transcription factor Foxa2 in lung cancer through epigenetic silencing." Lung Cancer.

Belinsky, S. A. (2004). "Gene-promoter hypermethylation as a biomarker in lung cancer." Nature Reviews Cancer **4**(9): 707-717.

Berge, G., S. Mollerup, et al. (2004). "Role of estrogen receptor in regulation of polycyclic aromatic hydrocarbon metabolic activation in lung." Lung Cancer **45**(3): 289-297.

Bernardo, G. M. and R. A. Keri (2012). "FOXA1: A transcription factor with parallel functions in development and cancer." Bioscience Reports **32**(2): 113-130.

Carroll, J. S., X. S. Liu, et al. (2005). "Chromosome-wide mapping of estrogen receptor binding reveals long-range regulation requiring the forkhead protein FoxA1." Cell **122**(1): 33-43.

Caruso, J. A., D. W. Laird, et al. (1999). "Role of HSP90 in mediating cross-talk between the estrogen receptor and the Ah receptor signal transduction pathways." Biochem Pharmacol **58**(9): 1395-1403.

Chand, A. L., D. D. Wijayakumara, et al. (2012). "The orphan nuclear receptor LRH-1 and ERα activate GREB1 expression to induce breast cancer cell proliferation." PLoS One **7**(2).

Chuang, J. C. and P. A. Jones (2007). "Epigenetics and microRNAs." Pediatric Research **61**(5 PART 2 SUPPL.): 24R-29R.

Damiani, L. A., C. M. Yingling, et al. (2008). "Carcinogen-induced gene promoter hypermethylation is mediated by DNMT1 and causal for transformation of immortalized bronchial epithelial cells." Cancer Res **68**(21): 9005-9014.

Enright, A. J., B. John, et al. (2003). "MicroRNA targets in Drosophila." Genome biology **5**(1).

Gazdar, A. F., B. Gao, et al. (2010). "Lung cancer cell lines: Useless artifacts or invaluable tools for medical science?" Lung Cancer **68**(3): 309-318.

Hanahan, D. and R. A. Weinberg (2000). "The hallmarks of cancer." Cell **100**(1): 57-70.

Hanahan, D. and R. A. Weinberg (2011). "Hallmarks of cancer: The next generation." Cell **144**(5): 646-674.

Harris, C. C. (1991). "Chemical and physical carcinogenesis: advances and perspectives for the 1990s." Cancer Res **51**(18 Suppl): 5023s-5044s.

Haugen, A. (2002). "Women who smoke: Are women more susceptible to tobacco induced lung cancer?" Carcinogenesis **23**(2): 227-229.

Hecht, S. S. (1998). "Biochemistry, biology, and carcinogenicity of tobacco-specific N-nitrosamines." Chemical Research in Toxicology **11**(6): 559-603.

Jacquet, M., V. Lambert, et al. (1996). "Correlation between P450 CYP1A1 inducibility, MspI genotype and lung cancer incidence." European Journal of Cancer Part A **32**(10): 1701-1706.

Jemal, A., F. Bray, et al. (2011). "Global cancer statistics." CA Cancer J Clin **61**(2): 69-90.

Jones, P. A. and S. B. Baylin (2007). "The Epigenomics of Cancer." Cell **128**(4): 683-692.

Kalluri, R. and R. A. Weinberg (2009). "The basics of epithelial-mesenchymal transition." Journal of Clinical Investigation **119**(6): 1420-1428.

Ke, X. S., Y. Qu, et al. (2008). "Epithelial to mesenchymal transition of a primary prostate cell line with switches of cell adhesion modules but without malignant transformation." PLoS One **3**(10).

Kongsuwan, K., M. R. Knox, et al. "The effect of combination treatment with trenbolone acetate and estradiol-17β on skeletal muscle expression and plasma concentrations of oxytocin in sheep." Domestic Animal Endocrinology(0).

Kure, E. H., D. Ryberg, et al. (1996). "p53 mutations in lung tumours: Relationship to gender and lung DNA adduct levels." Carcinogenesis **17**(10): 2201-2205.

Li, Z., G. Tuteja, et al. (2012). "Foxa1 and Foxa2 are essential for sexual dimorphism in liver cancer." Cell **148**(1-2): 72-83.

Lin, L., C. T. Miller, et al. (2002). "The hepatocyte nuclear factor 3 α gene, HNF3α (FOXA1), on chromosome band 14q13 is amplified and overexpressed in esophageal and lung adenocarcinomas." Cancer Research **62**(18): 5273-5279.

Lynam-Lennon, N., S. G. Maher, et al. (2009). "The roles of microRNA in cancer and apoptosis." Biological Reviews **84**(1): 55-71.

Ma, C., C. Hsu, et al. (2008). "Androgen Receptor Is a New Potential Therapeutic Target for the Treatment of Hepatocellular Carcinoma." Gastroenterology **135**(3): 947-955.e945.

Mani, S. A., W. Guo, et al. (2008). "The Epithelial-Mesenchymal Transition Generates Cells with Properties of Stem Cells." Cell **133**(4): 704-715.

Martello, G., A. Rosato, et al. (2010). "A microRNA targeting dicer for metastasis control." Cell **141**(7): 1195-1207.

Mattson, M. E., E. S. Pollack, et al. (1987). "What are the odds that smoking will kill you?" American Journal of Public Health **77**(4): 425-431.

McLemore, T. L., S. Adelberg, et al. (1990). "Expression of CYP1A1 gene in patients with lung cancer: evidence for cigarette smoke-induced gene expression in normal lung tissue and for altered gene regulation in primary pulmonary carcinomas." J Natl Cancer Inst **82**(16): 1333-1339.

Mollerup, S., G. Berge, et al. (2006). "Sex differences in risk of lung cancer: Expression of genes in the PAH bioactivation pathway in relation to smoking and bulky DNA adducts." Int J Cancer **119**(4): 741-744.

Mollerup, S., K. Jorgensen, et al. (2002). "Expression of estrogen receptors alpha and beta in human lung tissue and cell lines." Lung Cancer **37**(2): 153-159.

Mollerup, S., D. Ryberg, et al. (1999). "Sex differences in lung CYP1A1 expression and DNA adduct levels among lung cancer patients." Cancer Res **59**(14): 3317-3320.

Parkin, D. M., F. Bray, et al. (2005). "Global cancer statistics, 2002." CA Cancer J Clin **55**(2): 74-108.

Pfeifer, G. P., M. F. Denissenko, et al. (2002). "Tobacco smoke carcinogens, DNA damage and p53 mutations in smoking-associated cancers." Oncogene **21**(48): 7435-7451.

Ramirez, R. D., S. Sheridan, et al. (2004). "Immortalization of human bronchial epithelial cells in the absence of viral oncoproteins." Cancer Res **64**(24): 9027-9034.

Reddel, R. R., Y. Ke, et al. (1988). "Transformation of human bronchial epithelial cells by infection with SV40 or adenovirus-12 SV40 hybrid virus, or transfection via strontium phosphate coprecipitation with a plasmid containing SV40 early region genes." Cancer Research **48**(7): 1904-1909.

Sagredo, C., S. Mollerup, et al. (2009). "Biotransformation of benzo[a]pyrene in ahr knockout mice is dependent on time and route of exposure." Chemical Research in Toxicology **22**(3): 584-591.

Sagredo, C., S. Ovrebo, et al. (2006). "Quantitative analysis of benzo[a]pyrene biotransformation and adduct formation in Ahr knockout mice." Toxicol Lett **167**(3): 173-182.

Sharma, S., T. K. Kelly, et al. (2010). "Epigenetics in cancer." Carcinogenesis **31**(1): 27-36.

Shimizu, Y., Y. Nakatsuru, et al. (2000). "Benzo[a]pyrene carcinogenicity is lost in mice lacking the aryl hydrocarbon receptor." Proceedings of the National Academy of Sciences of the United States of America **97**(2): 779-782.

Siegfried, J. M., P. A. Hershberger, et al. (2009). "Estrogen receptor signaling in lung cancer." Semin Oncol **36**(6): 524-531.
Song, Y., M. K. Washington, et al. (2010). "Loss of FOXA1/2 is essential for the epithelial-to-mesenchymal transition in pancreatic cancer." Cancer Research **70**(5): 2115-2125.
Spink, D. C., B. H. Katz, et al. (2003). "Estrogen regulates Ah responsiveness in MCF-7 breast cancer cells." Carcinogenesis **24**(12): 1941-1950.
Subramanian, J. and R. Govindan (2007). "Lung cancer in never smokers: A review." Journal of Clinical Oncology **25**(5): 561-570.
Tang, Y., G. Shu, et al. (2011). "FOXA2 functions as a suppressor of tumor metastasis by inhibition of epithelial-to-mesenchymal transition in human lung cancers." Cell Research **21**(2): 316-326.
Tellez, C. S., D. E. Juri, et al. (2011). "EMT and stem cell-like properties associated with miR-205 and miR-200 epigenetic silencing are early manifestations during carcinogen-induced transformation of human lung epithelial cells." Cancer Research **71**(8): 3087-3097.
Thomsen, J. S., X. Wang, et al. (1994). "Restoration of aryl hydrocarbon (Ah) responsiveness in MDA-MB-231 human breast cancer cells by transient expression of the estrogen receptor." Carcinogenesis **15**(5): 933-937.
Tian, J., Z. Tu, et al. (2012). ERβ regulates miR-21 expression and inhibits invasion and metastasis in cancer cells.
Uppstad, H., S. Ovrebo, et al. (2010). "Importance of CYP1A1 and CYP1B1 in bioactivation of benzo[a]pyrene in human lung cell lines." Toxicol Lett **192**(2): 221-228.
Veglia, F., G. Matullo, et al. (2003). "Bulky DNA adducts and risk of cancer: a meta-analysis." Cancer Epidemiol Biomarkers Prev **12**(2): 157-160.
Veljkovic, E., J. Jiricny, et al. (2011). "Chronic exposure to cigarette smoke condensate in vitro induces epithelial to mesenchymal transition-like changes in human bronchial epithelial cells, BEAS-2B." Toxicology in Vitro **25**(2): 446-453.
Vogelstein, B. and K. W. Kinzler (2004). "Cancer genes and the pathways they control." Nat Med **10**(8): 789-799.
Yager, J. D. and N. E. Davidson (2006). "Estrogen carcinogenesis in breast cancer." New England Journal of Medicine **354**(3): 270-282+228.
Youlden, D. R., S. M. Cramb, et al. (2008). "The International Epidemiology of Lung Cancer: geographical distribution and secular trends." J Thorac Oncol **3**(8): 819-831.
Zang, E. A. and E. L. Wynder (1996). "Differences in lung cancer risk between men and women: examination of the evidence." J Natl Cancer Inst **88**(3-4): 183-192.
Zhang, J. Y., Y. F. Wang, et al. (2006). "Xenobiotic-metabolizing enzymes in human lung." Current Drug Metabolism **7**(8): 939-948.
Zhu, B. T. (2010). "On the general mechanism of selective induction of cytochrome P450 enzymes by chemicals: some theoretical considerations." Expert Opin Drug Metab Toxicol **6**(4): 483-494.

Appendix

Content

A. General cell culture work
B. CellTiter Blue – Fluorescence and number of cells
C. RNA quality – Agilent Bioanalyzer
D. Agarose gel electrophoresis
E. RT-qPCR results of *CYP1A1, CYP1B1* and *AHR* expression.
F. DNA methylation assay
G. Solutions

A. General cell culture work

Thawing cells

Materials

- Centrifuge (Eppendorf 5702)
- Light microscope (Nikon Diaphoto)

Reagents

- Growth medium
- DNAse
- Trypsin

Protocol

1. An ampoule was taken from the nitrogen tank and thawed in water bath (37 °C)
2. The cells were transferred to a centrifuge tube and 5 ml media was slowly added.
3. The tube was centrifuged (1000 rpm, 4 minutes)
4. The supernatant was removed and the pellet was re-suspended in 3 ml medium.
5. The cell suspension was pipette into a petridish (100mm) already containing 5 ml of medium (8 ml in total)
6. The petridish was incubated at 37 °C

Passaging cells

Protocol

1. The media over the cells was removed.
2. The cells were washed twice in 8 ml PBS.
3. 1 ml trypsin was added to the dish, and the cells were incubated for five minutes in incubator locker until the cells had loosened. This was checked in the microscope.
4. 5 ml media was added and pipette up and down to separate cells, and the cells were transferred to a centrifuge tube and centrifugated (1000 rpm, 4 minutes)

5. The supernatant was removed and treated with DNAse to facilitate separating the cells.
6. The pellet was re-suspended in medium. Amount of medium used depended on the desired dilution of the cells.
7. Cell suspension (1 ml) was pipetted to a new petridish added 7 ml medium (8 ml in total)
8. Cells were incubated in 37 °C

Freezing cells

Protocol

1. The protocol for passaging of cells was followed to point number 5.
2. The cell pellet was re-suspended in 500 µL freezing medium (AF solution) and transferred to a twist top vial.
3. 500 µL DMSO freezing media solution for cell culture storage was added and the suspension was mixed well.
4. The vial was put in an insulated box and placed at -80°C for 4 to 6 hours and then placed in STAMIs liquid nitrogen cell bank for a long-term storage.

Collagen coating of petridishes or cell culture plates

Protocol

1. Purified collagen solution for cell culture was diluted in PBS to a total concentration of 0.03 mg/ml
2. 3 ml was added 100 mm dishes, 1 ml to each well in 24-wells plates, 500 µL to 24-well plates and 100 µL to 96-well plates so that the dishes/plates were completely covered.
3. The dishes/plates were incubated at room temperature in the LAF bench for 2 hours.
4. The collagen solution was removed and the dishes were washed with PBS.

B. CellTiter Blue assay – Fluorescence and number of cells

This diagram shows the relationship between number of cell and fluorescence.

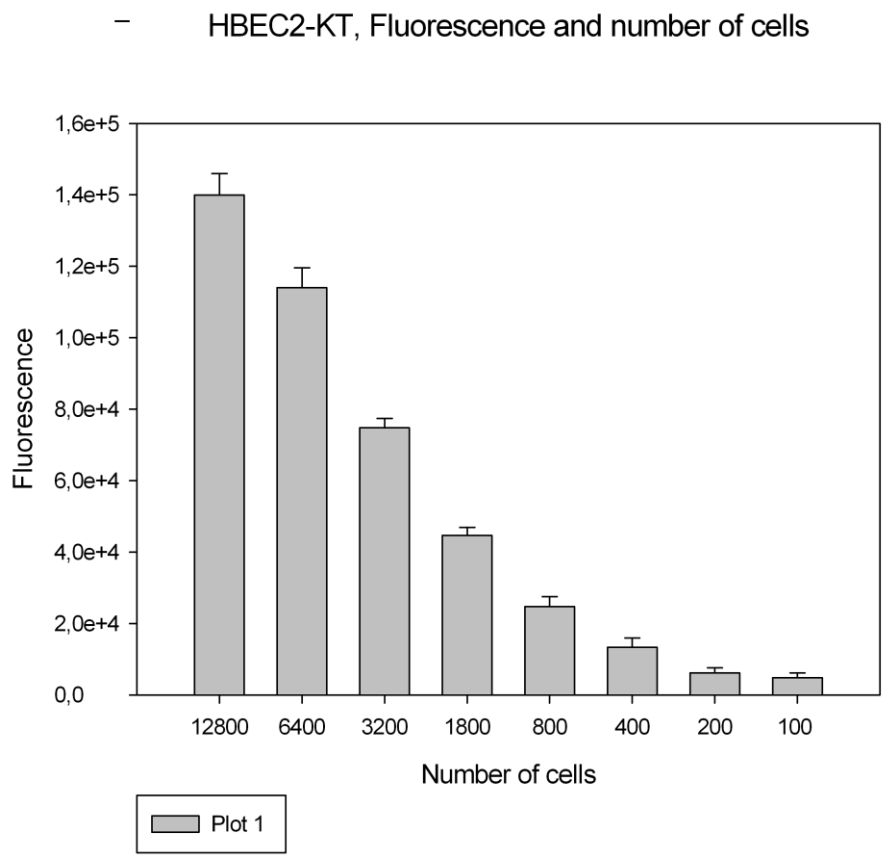

Figure B: Diagram showing the relationship between number of cells and fluorescence. Columns show the mean value SD.

C. RNA quality - Agilent Bioanalyzer

Agilent RNA kits are designed for the analysis of total RNA and mRNA samples.

Materials	**Reagents**
RNA nano chip electrode cleaners	Agilent RNA 6000 Ladder RNA Nano Dye Concentrate
Agilent 2100 Bioanalyzer instrument	Agilent RNA 6000 Nano Marker
Centrifuge (Eppendorf Centrifuge 5417R)	Agilent RNA 6000 Nano Gel Matrix
Heating block (Grant QBT2)	Spin filters
Micro centrifuge tubes (Trefflab)	DEPC water
RNAseZAP (Ambion, Inc. cat.no.9780)	

Protocol

1. A 200 ng/uL solution was made of all RNA samples. All RNA samples were denatured at 70°C before use.
2. The gel was prepared
   a. 550 µL of RNA 6000 Nano gel matrix was pipetted into a spin filter.
   b. This was centrifugated at 1500 g for 10 minutes at room temperature.
   c. 65 µL filtered gel was aliquoted into 0.5 ml micro centrifuge tubes
3. The Gel-Dye Mix was prepared
   a. The RNA 6000 Nano dye concentrate was allowed to equilibrate to room temperature for 30 minutes.
   b. RNA 6000 Nano dye concentrate was vortexed for 10 seconds, spinned down, and added 1 uL of dye into a 65 µL of filtered gel.

c. The solution was vortexed well. The tube was spinned at 13000 g for 10 minutes at room temperature.

4. The Gel-Dye Mix was loaded
   a. A new RNA 6000 Nano chip was put on the chip priming station.
   b. 9.0 µL of gel-dye mix was pipetted in the well marked (G)
   c. The chip priming station was closed after it was made sure that the plunger was positioned at the one ml position.
   d. The plunger was pressed until it was held by the chip
   e. After 30 seconds the chip was released
   f. After 5 seconds, the plunger was slowly pulled back to 1 ml position.
   g. The chip priming station was opened, and 9.0 µL of gel-dye mix was pipetted in the wells marked (G).
   h. The remaining gel dye mix was discarded.
5. The Agilent RNA 6000 Nano Marker was loaded
   a. 5 µL of the RNA 6000 Nano Marker was pipetted in all 12 sample wells and in the well marked for ladder.
6. The ladder and samples were loaded
   a. 1 uL of prepared ladder was pipette in the well marked ladder.
   b. 1 uL of sample was pipetted in each of the 12 sample wells. 1 µL of RNA 6000 Nano Marker was pipetted in each unused sample well.
   c. The chip was put horizontally in the adapter of the IKA vortexer and vortexed for 1 minute at 2400 rpm.
   d. The chip was runned within 5 minutes in the Agilent 2100 bioanalyzer.

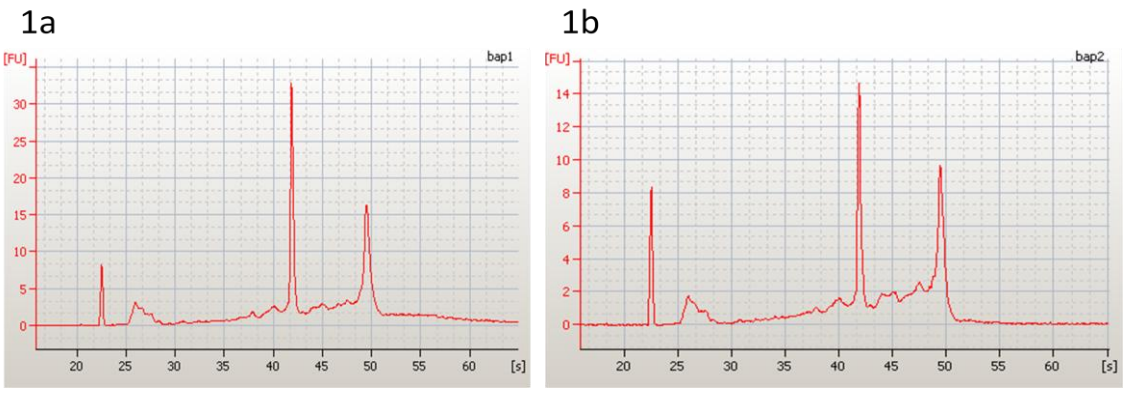

Figure C: 1a and 1b) Shows the results from HBEC cells treated with 1 uM B[*a*]P.

D. Agarose gel electrophoresis

Agarose gel electrophoresis can be used to separate DNA molecules. This was used to test that the primers had correct length and that there was only one product. A gel concentration of 3 % (NuSieve gel) was used at 120 V for 90 minutes. Figure D shows the results from *CDH1, CDH2, FOXA1* and *GREB1.*

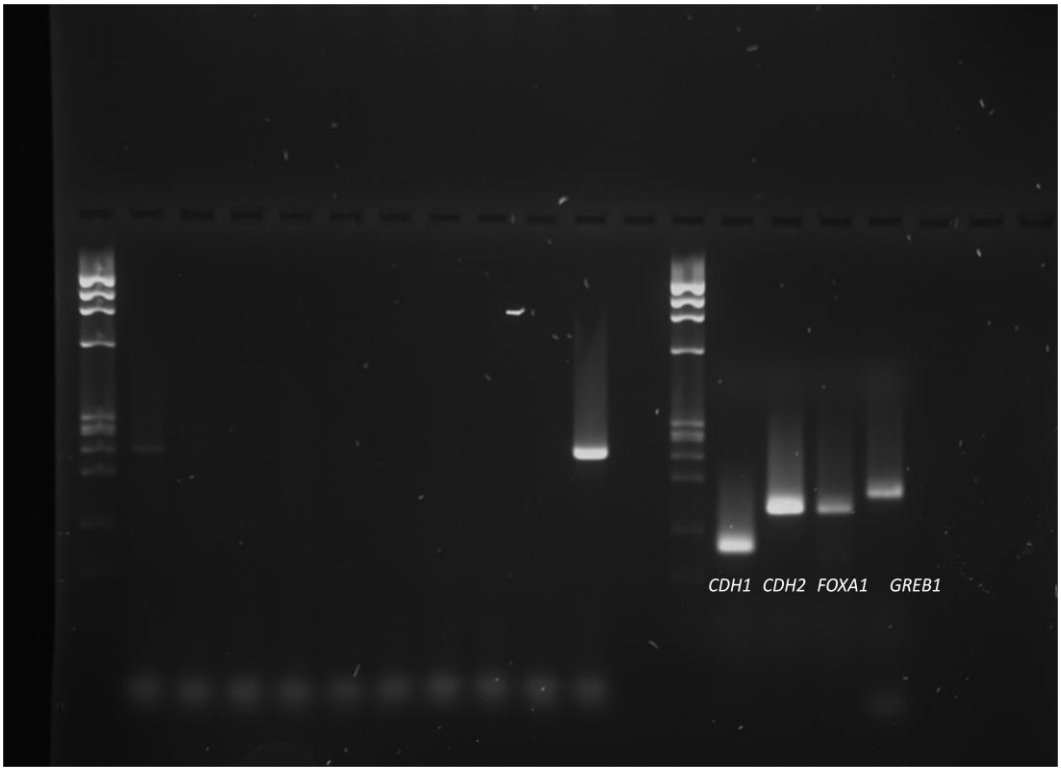

Figure D: Result from Agarose gel electrophoresis.

E. RT-qPCR results of *CYP1A1, CYP1B1* and *AHR.*

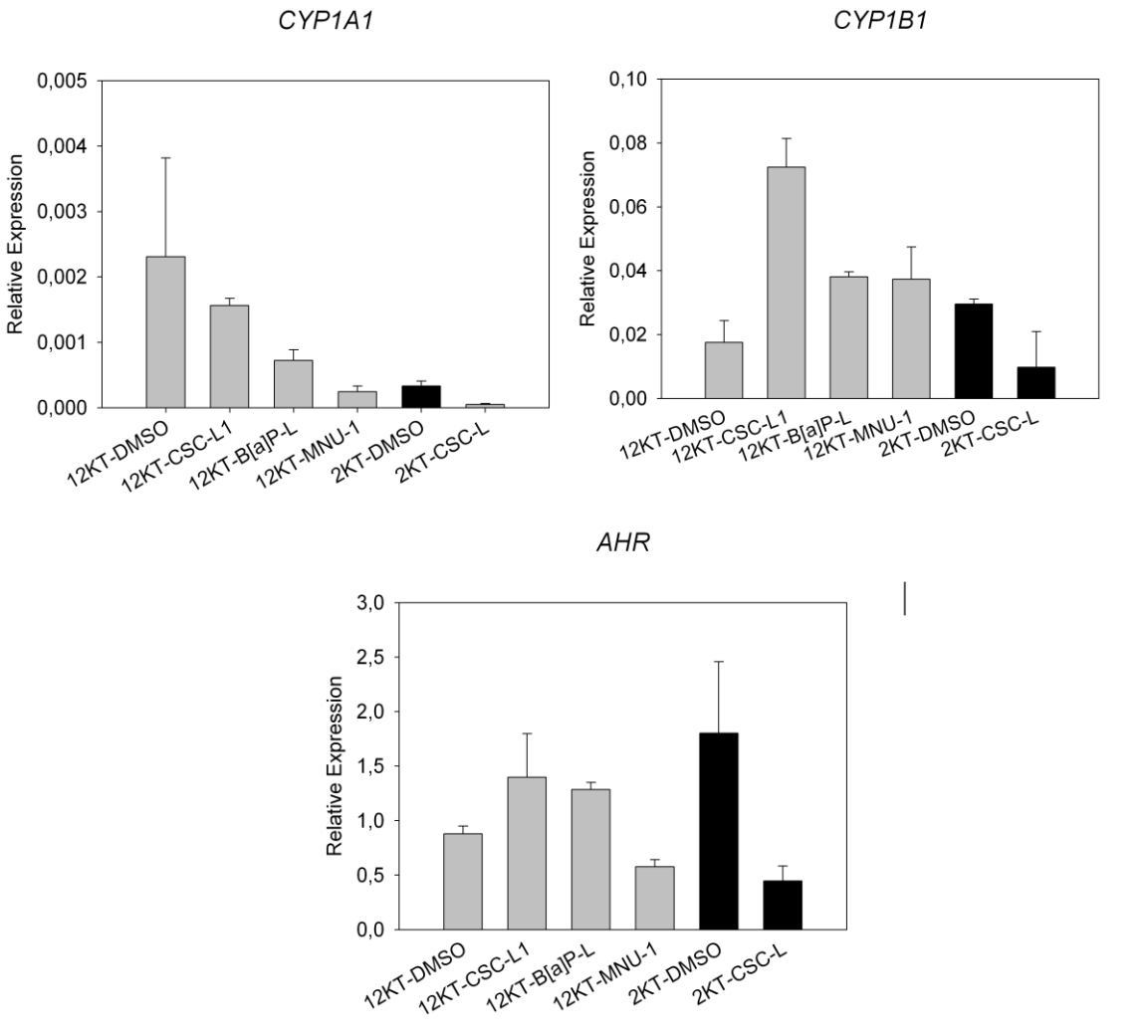

Figure E: Columns show the mean value SD. Results from qPCR on four transformed cell lines. HBEC-12KT derived cell lines are in grey, and HBEC-2KT derived cells are in black.

F. DNA methylation assay

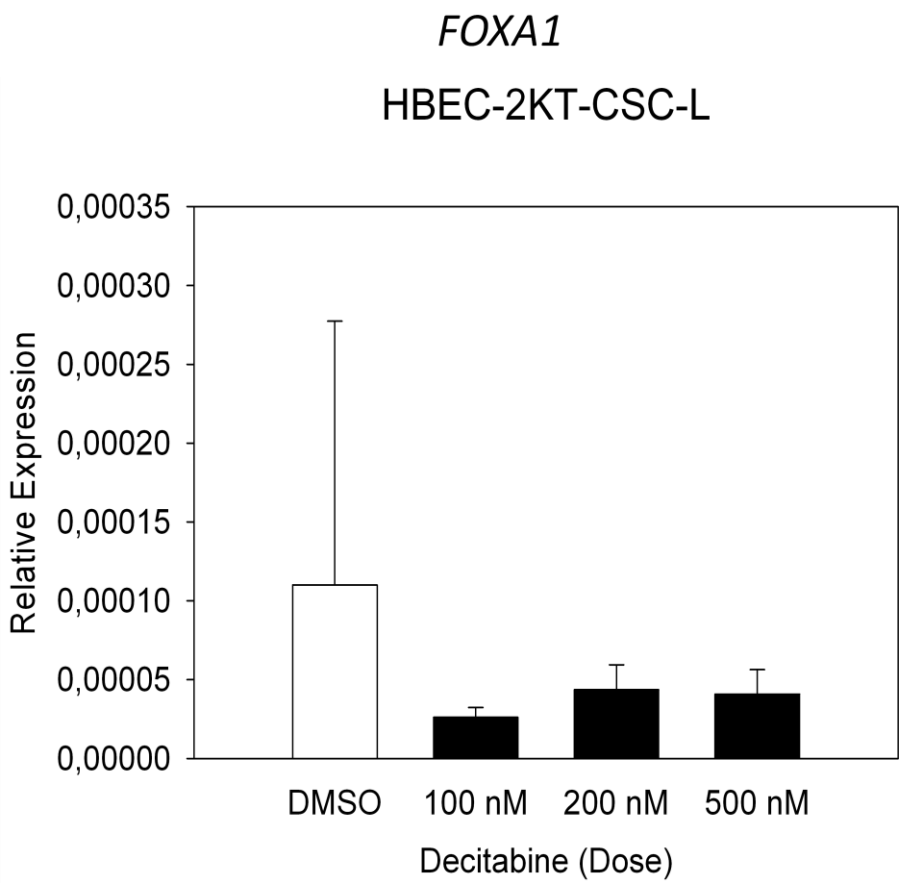

Figure F: Columns show the mean value SD.

G. Solutions

AF- medium (Antibiotic freezing medium)

- 76% L-15 medium
- 2% 1M HEPES
- 2% PS
- 20% FBS

The solution was sterilefiltered and stored at -4°C.

DEPC water

Diethylpyrocarbonate (DEPC) was added distilled water (ddH_2O) to obtain a 0.1% DEPC water solution.

DMSO (dimethylsulfoxide) for cell culture storage

- 50 % L-15 medium
- 2 % 1M HEPES
- 8 % DMSO
- 40 % FBS

The solution was sterile-filtered and stored at -4 °C.

DNAse (4mg/ml)

- 4 g DNAse
- 87.66 mg NaCl
- 5.06 mg $MgSO_4$
- H_2O to 1 ml

The solution was stored at -4°C.

Ethanol in DEPC water (75%)

12.5 DEPC water, absolute ethanol to 50 ml. The solution was stored in the fridge.

Fetal Bovine Serum (FBS)

The serum was heat inactivated at 56 °C for 45 minutes and stored at -4 °C.

HEPES

- 238.3 g HEPES
- 1 ml 0.12% phenol red in 1 L ddH_2O, pH 7.3

Phenol red

- 125 g phenol red
- 360 µL 1M NaOH
- 100 ml H_2O

Phosphate buffered saline (PBS)

- 7.07 g NaCl
- 0.20 g KCl
- 1.94 g $NaHPO_4 \cdot H_2O$
- H_2O to 1 L.